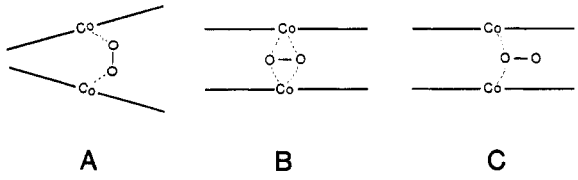

Figure 7. Three different modes of O_2 binding suggested for μ-superoxo complex of four-atom-bridged cofacial dimer.

Another interesting property of the Co_2(FTF4) system is the existence of a stable mixed-valence state, Co^{III} Co^{II},[19] which now seems to be a consequence of the very short distance that promotes a strong interaction between the two nearly equivalent Co centers. The mixed-valence complex exhibits a very high O_2 affinity and forms a stable O_2^- (μ-superoxo) complex.[20] The role of this stable O_2^- complex in the catalytic O_2 reduction is not fully understood, but its structure may further clarify the mechanism of this important process. Several years ago from the shape of the EPR spectrum of the μ-superoxo complex, Chang and Wang proposed[21] that, in the four-atom-bridged dimer, dioxygen binds in a cis fashion (structure A in Figure 7). A theoretical study[22] suggests that such a cis structure may exist if steric constraints allow it. However, the present structure does not seem to support this hypothesis since enormous steric repulsion would result as the two porphyrin rings approach one another on one side to accommodate a cis-bound O_2 complex. Instead, we suspect dioxygen may be bound between the Co centers parallel to the porphyrin rings either symmetrically (structure B) or asymmetrically (structure C in Figure 7). Although neither of these O_2 binding modes has been observed in transition-metal complexes,[23] structure B was once proposed in a theoretical study[24] for $[(H_3N)_5Co]_2O_2^{5+}$. Structure C is attractive since it makes the coordinated O_2 molecule more susceptible to protonation. Recently we isolated[5] the O_2 complexes of Co_2(FTF4) and Co_2(DPB), but thus far we have not been able to grow single crystals suitable for X-ray diffraction study. Therefore, the nature of O_2 bonding in these complexes remains unresolved at this time.

Acknowledgment. We thank Dr. M. G. Finn and Professor Brian M. Hoffman for helpful discussions. This work was kindly supported by the National Institutes of Health (HL-13157, JAI; 5R01-NIHGM17880-15,16, JPC) and by the National Science Foundation (NSF CHE83-18512, JPC).

Registry No. Co_2(FTF4)·CH_3OH·1.6CH_2Cl_2, 114221-01-1.

Supplementary Material Available: Positional and equivalent isotropic thermal parameters for non-hydrogen atoms (Table SI), anisotropic thermal parameters (Table SII), hydrogen-atom parameters (Table SIV), and least-squares planes and dihedral angles between the least-squares planes (Table SV) (4 pages); listing of observed and calculated structure amplitudes (Table SIII) (13 pages). Ordering information is given on any current masthead page.

(19) Le Mest, Y.; L'Her, M.; Courtot-Coupez, J.; Collman, J. P.; Evitt, E. R.; Bencosme, C. S. *J. Electroanal. Chem.* **1985**, *184*, 331-346.
(20) (a) Le Mest, Y.; L'Her, M.; Courtot-Coupex, J.; Collman, J. P.; Evitt, E. R.; Bencosme, C. S. *J. Chem. Soc., Chem. Commun.* **1983**, 1286-1287. (b) Le Mest, Y.; L'Her, M.; Collman, J. P. Hendricks, N. H.; McElwee-White, L. *J. Am. Chem. Soc.* **1986**, *108*, 533-535.
(21) Change, C. K.; Wang, C.-B. In *Electron Transport and Oxygen Utilization*; Ho, C., Ed.; Elsevier: Amsterdam, 1982;f pp 237-243.
(22) Tatsumi, K.; Hoffmann, R. *J. Am. Chem. Soc.* **1981**, *103*, 3328-3341.
(23) The symmetrically bridging side-on coordination geometry of dioxygen (Structure B) has been observed in a uranium complex. Boeyens, J. C. A.; Haegele, R. *J. Chem. Soc., Dalton Trans.* **1977**, 648-650.
(24) Vlček, A. A. *Trans. Faraday Soc.* **1960**, *56*, 1137-1143.

Synthesis of an (η^3-Allyl)(hydrido)iridium Complex and Its Reactions with Arenes and Alkanes. Sequential Intermolecular C-H Oxidative Addition and Hydride-to-Alkene Migratory Insertion Reactions

William D. McGhee and Robert G. Bergman*

Contribution from the Materials and Chemical Sciences Division, Lawrence Berkeley Laboratory, and the Department of Chemistry, University of California, Berkeley, California 94720.
Received November 2, 1987

Abstract: The iridium allyl hydride complex (η^5-C_5Me_5)(η^3-C_3H_5)(H)Ir (**2**) has been prepared from $[(\eta^5\text{-}C_5Me_5)IrCl_2]_2$, and its reaction with arenes and alkanes has been investigated. The hydride reacts with C-H bonds in benzene and cyclopropane in the presence of phosphines L, leading to the phenyl and cyclopropyl complexes (η^5-C_5Me_5)(L)Ir(*n*-propyl)(R) (**3**, **4**, and **5**). Irradiation of **2** in the presence of PMe_3 takes a different course, giving the previously uncharacterized (η^5-C_5Me_5)Ir(PMe_3)$_2$ (**6**). Thermal reaction of **2** in alkane solvents such as *n*-butane and isobutane, which are capable of β-elimination, leads to products **8a**, **8b**, and **9** formed by replacement of the allyl group in **2** by a substituted allyl ligand formed by overall dehydrogenation of the alkane. Thermolysis of **2** in the presence of arenes such as *n*-propylbenzene and cumene leads to more complicated products resulting from intermolecular C-H activation followed by cyclometalation (e.g., **13**, **15**) and/or dimerization (**20**). The structure of cyclometalated dimer **20** has been determined by X-ray diffraction. Mechanistic studies, including kinetics, isotope tracer experiments, and intra- versus intermolecular isotope effect determinations, implicate the coordinatively unsaturated species (η^5-C_5Me_5)(η^2-propene)Ir (complex A in Scheme XX) as the initially formed intermediate in the thermal reactions of **1** with alkanes and arenes. Significant differences exist between the behavior of this intermediate (cf. Schemes XIX and XXIII) and that of the closely related phosphine-substituted complex (η^5-C_5Me_5)(PMe_3)Ir studied earlier; possible reasons for these differences are discussed.

Many examples are now known of C-H activation by soluble transition-metal complexes.[1] In only a few systems, however, has the product of C-H insertion been converted, either stoichiometrically or catalytically, into functionalized organic prod-

0002-7863/88/1510-4246$01.50/0

Scheme I

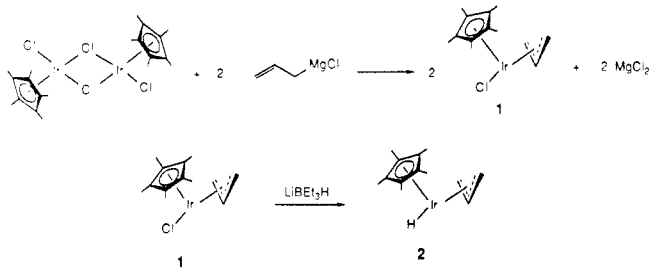

Scheme II

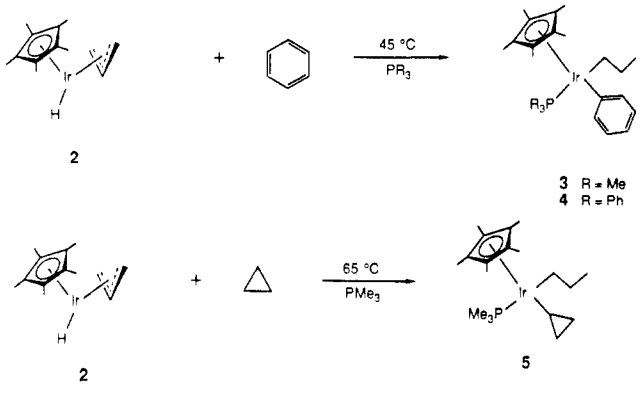

ucts.[2] In one potential functionalization scheme, C–H oxidative addition (eq 1) might be followed by insertion of another metal-bound ligand X into the new M–C or M–H bond (eq 2). Reductive elimination of the inserted ligand (eq 3) would then lead to the functionalized molecule R–X–H.

$$M\text{–}X + R\text{–}H \rightarrow X\text{–}M(H)(R) \quad (1)$$

$$X\text{–}M(H)(R) \rightarrow R\text{–}X\text{–}M\text{–}H \quad (2)$$

$$R\text{–}X\text{–}M\text{–}H \rightarrow M + R\text{–}X\text{–}H \quad (3)$$

The C–H oxidative addition step, once thought to be very difficult, is now a well-established process. However, completion of the functionalization scheme has been frustrated in many systems by the unfavorable relative rates of reaction 2 and the reverse of reaction 1. That is, the rate of reductive elimination of R–H to regenerate alkane is often substantially greater than that of insertion of the metal-bound hydrogen or alkyl group into the M–X bond. This has been a particularly difficult problem with third-row metals such as iridium, where insertion reactions involving polar dative ligands such as CO are extremely slow.[3] In order to develop a system in which eq 2 might be feasible, we decided to search for C–H oxidative addition reactions at metal centers having olefinic ligands coordinated to them, in hopes that the metal-bound hydrogen would migrate to these ligands more rapidly than R–H elimination occurs. In this paper the full details of a system which operates in this way are reported.

Results

Synthesis of (η^5-C_5Me_5)Ir(η^3-C_3H_5)H (Scheme I). Addition of allylmagnesium chloride to $[(\eta^5\text{-}C_5Me_5)IrCl_2]_2$[4] in diethyl ether

Scheme III

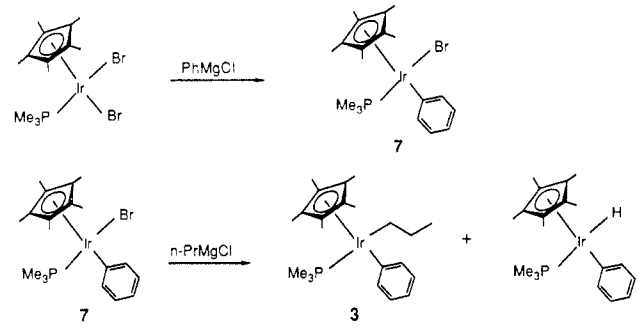

gave (η^5-C_5Me_5)Ir(η^3-C_3H_5)Cl (**1**), in typically 55–80% yields as yellow air stable needles. Reactions of **1** with $LiBEt_3H$ yielded a highly air sensitive, analytically pure white solid in 54–62% yield. On the basis of spectroscopic and analytical data (see Experimental Section) the formula of this product is assigned as (η^5-C_5Me_5)-Ir(η^3-C_3H_5)H (**2**).[5] These data also support a proposed structure having a static η^3-C_3H_5 group and a terminal hydride. In the solid-state infrared spectrum an Ir–H stretch is observed at 2095 cm^{-1} and in the solution ^1H NMR spectrum the hydride resonance is at δ –16.7 (C_6D_6), supporting the presence of an Ir–H linkage. The hydride is coupled to only one set of α-allyl protons (J_{HH} = 3.5 Hz).[6] The π-allyl hydrogens, in addition to the small hydride coupling, appear as a simple A_2B_2X spin system with no observable geminal coupling between the *syn*- and *anti*-allyl protons. In the ^{13}C NMR spectrum (C_6D_6) the allylic carbons appear at δ 20.6 (t, J_{CH} = 150 Hz) and δ 64.9 (d, J_{CH} = 162 Hz), showing no observable coupling between the hydride proton and either the α- or β-allylic carbons.

Reaction of Allyl Hydride 2 with Benzene and Cyclopropane in the Presence of Phosphines (Scheme II). Heating a solution of **2** in C_6H_6 (ca. 0.01 M) with 1.5 equiv of PMe_3 to 45 °C for 14 h produced two new organometallic products in a ratio of 9:1. The major product was isolated in 62% yield; on the basis of spectral and analytical data (see below and Experimental Section) it was assigned as (η^5-C_5Me_5)Ir(PMe_3)(*n*-Pr)C_6H_5 (**3**). The minor product was identified as (η^5-C_5Me_5)Ir(PMe_3)$_2$ (**6**) (vida infra). Use of PPh_3 in place of PMe_3 in the above reaction yielded **4**, the PPh_3 analogue of **3**, as the sole product in 43–51% isolated yield.

In both **3** and the PPh_3 analogue **4**, the *n*-propyl group can be readily distinguished in the ^1H and ^{13}C NMR spectra from other possible ligands (i.e., isopropyl or hydride). In the ^1H NMR spectrum (C_6D_6 for **3**) the CH_3 portion of the propyl group appears as a triplet, δ 1.31 (J_{HH} = 6.4 Hz) and the CH_2 groups as complex multiplets. In the ^{13}C NMR spectrum of **3**, the *n*-propyl carbons appear as a quartet at δ 21.44 (J_{CH} = 125.6 Hz), a doublet of triplets at δ 30.11 (J_{CP} = 5.4 Hz, J_{CH} = 125.9 Hz), and a doublet of triplets at δ 5.20 (J_{CP} = 8.7 Hz, J_{CH} = 128 Hz). For **4** a similar pattern is seen in both the ^1H and ^{13}C NMR spectra for the *n*-propyl group.

The σ-phenyl ligand in **3** shows two sets of complex resonances in the ^1H NMR (C_6D_6) spectrum, δ 7.48–7.45 for the ortho

(1) For reviews see: (a) Shilov, A. E. *Activation of Saturated Hydrocarbons by Transition Metal Complexes*; D. Riedel Publishing Co.: Dordrecht, 1984. (b) Crabtree, R. H. *Chem. Rev.* **1985**, *85*, 245.

(2) (a) Periana, R. A.; Bergman, R. G. *J. Am. Chem. Soc.* **1986**, *108*, 7332. (b) Janowicz, A. H.; Bergman, R. G. *Ibid* **1983**, *105*, 3929. (c) Fisher, B. J.; Eisenberg, R. *Ibid.* **1986**, *108*, 535. (d) Kunin, A. J.; Eisenberg, R. *Organometallics* **1983**, *2*, 764. (e) Sakakura, T.; Tanaka, M. *J. Chem. Soc., Chem. Commun.* **1987**, 758. (f) Sakakura, T.; Tanaka, M. *Chem. Lett.* **1987**, 249. (g) Burk, M. J.; Crabtree, R. H.; McGrath, D. V. *J. Chem. Soc., Chem. Commun.* **1985**, 1829. (h) Baudry, D.; Ephritikhine, M.; Felkin, H.; Holmes-Smith, R. *J. Chem. Soc., Chem. Commun.* **1983**, 788. (i) Green, M. L. H.; Parkin, G. *Ibid.* **1984**, 1467.

(3) In (η^5-C_5Me_5)(CO)Ir(R)H, migration of R or H to the carbonyl was not observed. Hoyano, J. K.; Graham, W. A. G. *J. Am. Chem. Soc.* **1982**, *104*, 3723.

(4) Kang, J. W.; Moseley, K.; Maitlis, P. M. *J. Am. Chem. Soc.* **1969**, *91*, 5970.

(5) For examples of other π-allyl hydride complexes see: (a) Baudry, D.; Boydell, P.; Ephritikhine, M.; Felkins, H.; Guilhem, J.; Pascard, C.; Dau, E. T. H. *J. Chem. Soc., Chem. Commun.* **1985**, 670. (b) Baudry, D.; Cormier, J.; Ephritikhine, M.; Felkin, H. *J. Organomet. Chem.* **1984**, *277*, 99. (c) Thorn, D. L. *Organometallics* **1982**, *1*, 879. (d) Carturan, G.; Scrivanti, A.; Morandini, F. *Angew. Chem., Int. Ed. Engl.* **1981**, *20*, 112. (e) Howarth, O. W.; McAteer, C. H.; Moore, P.; Morris, G. E. *J. Chem. Soc., Chem. Commun.* **1981**, 506. (f) Tulip, T. H.; Ibers, J. A. *J. Am. Chem. Soc.* **1979**, *101*, 4201. (g) Sherman, E. O.; Olsen, M. *J. Organomet. Chem.* **1979**, *172*, C13. (h) Tulip, T. H.; Ibers, J. A. *J. Am. Chem. Soc.* **1978**, *100*, 3252. (i) Sherman, E. O.; Schreiher, P. R. *J. Chem. Soc., Chem. Commun.* **1978**, 223. (j) Byrne, J. W.; Blaser, H. U.; Osborn, J. A. *J. Am. Chem. Soc.* **1975**, *97*, 3871. (k) Nixon, J. F.; Wilkins, B. *J. Organomet. Chem.* **1974**, *80*, 129. (l) Bonnemann, H. *Angew. Chem., Int. Ed. Engl.* **1970**, *9*, 736. Portions of the work described here have been reported earlier in preliminary form: (m) McGhee, W. D.; Bergman, R. G. *J. Am. Chem. Soc.* **1985**, *107*, 3388.

(6) A small coupling between the hydride and the allylic hydrogens was also seen in the ^1H NMR spectrum of (η^3-C_3H_5)(PR_3)PtH: ref 5d.

Scheme IV

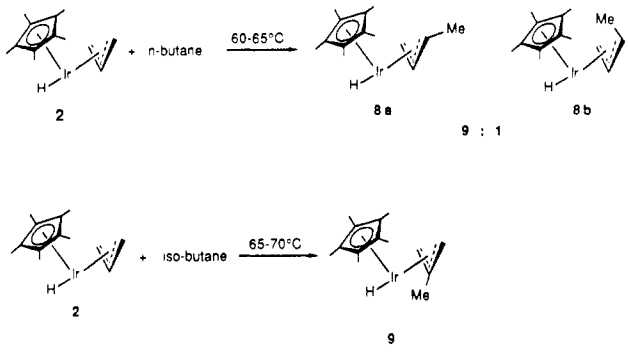

protons and δ 7.22–7.12 for the meta and para protons. For **4** the aromatic region is complicated due to the nature of the PPh_3 ligand. As seen in similar complexes, slow rotation of the PPh_3 ligand occurs at room temperature on the NMR time scale giving rise to broad peaks in the aromatic region.[7] Cooling a CD_2Cl_2 solution of **4** to −80 °C in the NMR probe freezes out the rotation; however, both the ^1H and $^{13}C\{^1H\}$ NMR spectra are extremely complex and complete assignment of peaks was not possible.

The mass spectra of both **3** and **4** are helpful in determining their identity. In both cases strong M^+ signals are seen (*m/e* 524 and 710, respectively). The major fragment in the mass spectra of these complexes is the parent ion minus the *n*-propyl group (*m/e* 481 and 667, respectively).

The use of cyclopropane in place of benzene as solvent gave the corresponding *n*-propyl(σ-cyclopropyl)iridium complex **5** (39%). The conditions for this reaction were slightly different; the reaction mixture was heated to 65 °C for 16.5 h (to prevent the formation of **6** the reaction vessel was protected from light (vida infra)). Again the information most helpful for standard assignment comes from the ^{13}C NMR (C_6D_6) and mass spectra. In the ^{13}C NMR spectrum the *n*-propyl carbons appear at δ 2.06 (dt, J_{CP} = 9 Hz, J_{CH} = 124 Hz), 21.68 (q, J_{CH} = 122 Hz), 30.98 (dt, J_{CP} = 4.9 Hz, J_{CH} = 121 Hz) and the cyclopropyl carbons appear at δ −29.4 (dd, J_{CP} = 13.5 Hz, J_{CH} = 148 Hz), 3.0 (t, J_{CH} = 155 Hz), 4.72 (t, J_{CH} = 156 Hz). In the mass spectrum the complex shows a strong M^+ at *m/e* 448.

Independent Synthesis of *n*-Propylphenyliridium Complex 3 (Scheme III). To further support the assignment of the above complexes the independent synthesis of **3** was carried out. PhMgCl was added dropwise to a slurry of $(\eta^5\text{-}C_5Me_5)Ir(PMe_3)Br_2$[8] in diethyl ether, giving yellow-orange crystals of $(\eta^5\text{-}C_5Me_5)Ir(PMe_3)(C_6H_5)Br$ (**7**) in 50–55% yields. Spectroscopically, **7** is similar to its known rhodium analogue.[7] Variable-temperature ^1H NMR (CD_2Cl_2) spectra of **7** were obtained, and from these data a value of 13.9 kcal mol^{-1} for $\Delta G°$ was calculated from the coalescence temperature for the rotation about the Ir–Ph bond. The value for the rhodium analogue was calculated[7] as 14 kcal mol^{-1}.

Addition of *n*-PrMgCl to bromophenyliridium complex **7** gave *n*-propylphenyliridium complex **3** and $(\eta^5\text{-}C_5Me_5)Ir(PMe_3)(Ph)H$ in a 1:1 ratio. These complexes were separated by chromatography on silica gel. By ^1H and $^{13}C\{^1H\}$ NMR spectroscopy, **3** synthesized in this manner was identical with the major product formed in the thermolysis reaction described above utilizing **2**, C_6H_6, and PMe_3.

Thermolysis of the Allyliridium Hydride 2 in *n*-Butane and Isobutane (Scheme IV). In a heavy-walled glass bomb a solution of **2** in *n*-butane was heated to 60–65 °C for 2 days. Sublimation led to the two isomers of $(\eta^5\text{-}C_5Me_5)Ir(\eta^3\text{-}1\text{-}MeC_3H_4)H$ (**8a** and **8b**) in a 9:1 ratio by ^1H NMR analysis. The *syn*-methyl isomer **8a** is the major product (vida infra). Similarly, heating **2** in isobutane (ca. 0.01 M) to 70–75 °C for 7 days gave a new complex in 12–14% isolated yield, which by ^1H NMR (C_6D_6) and solution IR spectroscopy (C_6D_6) was identified as $(\eta^5\text{-}C_5Me_5)Ir(\eta^3\text{-}2\text{-}MeC_3H_4)H$ (**9**) (vida infra).

Scheme V

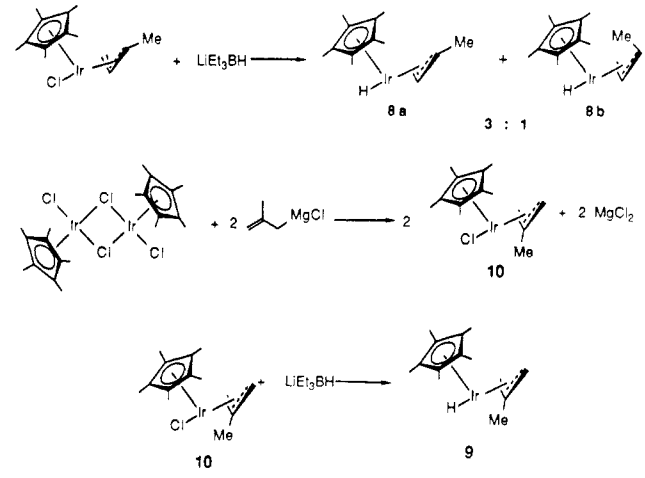

Scheme VI

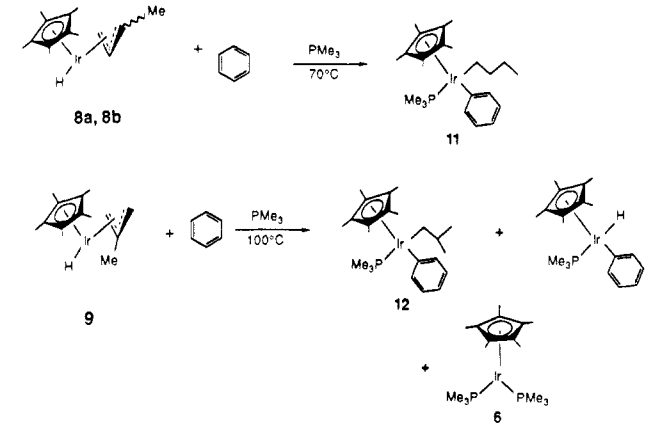

Confirmation of the above assignments was obtained by independent synthesis (Scheme V). Treatment of the known[9] $(\eta^5\text{-}C_5Me_5)Ir(\eta^3\text{-}1\text{-}MeC_3H_4)Cl$ with $LiBEt_3H$ in ether gave two products, having Ir–H resonances in the ^1H NMR spectrum at δ −17.28 and −17.02, in a relative ratio of 3:1. By ^1H (C_6D_6), $^{13}C\{^1H\}$, and ^{13}C (DEPT) NMR spectroscopy the two products were assigned as the *syn*- and *anti*-methallyl hydride complexes, **8a** and **8b**. The major product was assigned as the syn isomer based on the coupling constants between the α-allylic hydrogens and the β-allylic hydrogen. Heating the 3:1 mixture of stereoisomers **8a** and **8b** in C_6D_{12} or C_6H_6 to 85 °C for 1 h changed the ratio of isomers to 9:1. Continued heating did not alter the ratio any further. From these data K_{eq} = 9 and $\Delta G°$ = 1.5 kcal mol^{-1} for the syn–anti interconversion.

Synthesis of the chloro 2-methallyl complex **10** was achieved in 58% yield by addition of (2-methallyl)MgCl to a slurry of $[(\eta^5\text{-}C_5Me_5)IrCl_2]_2$ in diethyl ether. The chloride was converted to the corresponding hydride by the addition of $LiBEt_3H$; **9** was isolated in 83% yield as clear, air-sensitive crystals. As in **2**, a small coupling between the hydride and one set of α-allylic protons is observed (J_{HH} = 3.1 Hz).

Reaction of the Methylallyl Isomers 8a, 8b, and 9 with C_6H_6 in the Presence of PMe_3 (Scheme VI). In analogy to the reaction described between allyl hydride **2**, C_6H_6, and PMe_3, the 2-methallyl iridium complexes **8a**, **8b**, and **9** were each allowed to react with C_6H_6 in the presence of PMe_3. The relative rates of reaction varied qualitatively in the order **2** > **8a** and **8b** > **9**. For convenience the reaction between **8a** and **8b**, C_6H_6 and PMe_3 was carried out at 80 °C; this gave a 47% yield of clear analytically pure crystals of $(\eta^5\text{-}C_5Me_5)Ir(PMe_3)Ph(n\text{-}Bu)$ (**11**). Spectro-

(7) Jones, W. D.; Feher, F. J. *Inorg. Chem.* **1984**, *23*, 2376. See references therein for other examples of hindered rotation in organometallic complexes.

(8) Synthesized by metathesis of $(\eta^5\text{-}C_5Me_5)(PMe_3)IrCl_2$ (ref 4) with LiBr: Buchanan, J. M.; Bergman, R. G., unpublished results.

(9) Moseley, K.; Kang, J. W.; Maitlis, P. M. *J. Chem. Soc. A* **1970**, 2876.

Scheme VII

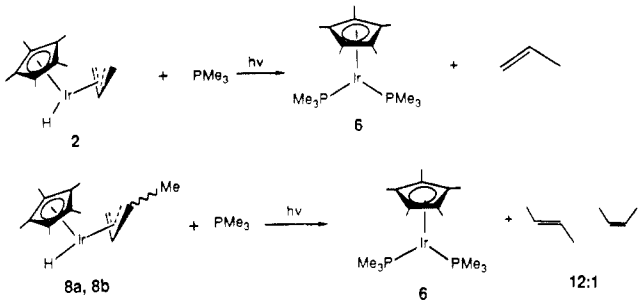

scopically **11** is similar to the *n*-propyl analogue **3**. In the $^{13}C\{^1H\}$ NMR spectrum (C_6D_6) the resonances due to the *n*-butyl carbons appear at δ 39.7 (d, J_{CP} = 4.3 Hz), 29.8, 15.6, and 1.63 (d, J_{CP} = 8.8 Hz). The mass spectrum of the *n*-butyl complex showed a parent ion at *m/e* 538 and $M^+ - C_4H_9$ at *m/e* 481. No indication of the *sec*-butyl isomer was observed. The reaction with **9**, C_6H_6, and PMe_3 was carried out preparatively at 100 °C. Analysis of the crude reaction mixture by ^1H NMR spectroscopy in this case showed 3 products in a ratio of 1:2:3.5 corresponding to $(\eta^5\text{-}C_5Me_5)Ir(PMe_3)_2$ (**6**), $(\eta^5\text{-}C_5Me_5)Ir(PMe_3)(Ph)H$, and $(\eta^5\text{-}C_5Me_5)Ir(PMe_3)(Ph)i\text{-}Bu$ (**12**). The isobutyl complex **12** was isolated in 24% yield by passage of the reaction mixture through alumina followed by two crystallizations from pentane at −40 °C. The isobutyl protons appear as two diastereotopic methyl doublets at δ 1.23 (J_{HH} = 6.1 Hz) and 1.15 (J_{HH} = 6.1 Hz) and complex one-proton multiplets at δ 1.6 and 1.8. In the $^{13}C\{^1H\}$ NMR spectrum (C_6D_6) the carbons due to the isobutyl group appear at δ 28.0, 27.1, 33.5 (d, J_{CP} = 4.7 Hz), and 12.3 (d, J_{CP} = 9.2 Hz). The mass spectrum of the isobutyl complex gave a M^+ at *m/e* 538 and $M^+ - C_4H_9$ at *m/e* 481.

Irradiation of Allyl Hydride 2 in the Presence of PMe_3: Synthesis of $(\eta^5\text{-}C_5Me_5)Ir(PMe_3)_2$ (Scheme VII). In view of the fact that $Cp'M(PMe_3)_2$ (Cp′ = $\eta^5\text{-}C_5H_5$, $\eta^5\text{-}C_5Me_5$, M = Co, Rh; and Cp′ = $\eta^5\text{-}C_5H_5$, M = Ir) are known,[10] it is peculiar that the corresponding iridium complex **6** has apparently not been reported previously. To provide a useful independent synthesis of this material either a hexane or benzene solution of the (π-allyl)iridium hydride **2** with 40 equiv of PMe_3 was irradiated for 5 h. Concentration of the resulting bright orange solution followed by crystallization gave a bright orange, highly air sensitive, analytically pure solid in 74% yield. On the basis of its spectral and analytical data the product is formulated as $(\eta^5\text{-}C_5Me_5)Ir(PMe_3)_2$ (**6**). Spectroscopically, **6** is similar to the other known $Cp'M(PMe_3)_2$ complexes.[9] The $\eta^5\text{-}C_5Me_5$ ligand appears as a triplet at δ 2.03 (t, J_{HP} = 1.2 Hz) and the PMe_3 ligands appear at δ 1.41 (virtual triplet $^2J_{HP} + {}^4J_{HP}$ = 8.6 Hz). The parent as well as base peak in the mass spectrum of **6** appears at *m/e* 480, corresponding to $(\eta^5\text{-}C_5Me_5)Ir(PMe_3)_2^{\bullet+}$. Monitoring the reaction by ^1H NMR spectroscopy (C_6D_6) showed the clean formation of **6** and the production of free propene. In a control experiment two identical C_6D_6 solutions of **2** with added PMe_3 were allowed to stand at room temperature, one under room light and the other in the dark. The reaction mixture exposed to the room light produced significant quantities of both the bis-phosphine complex **6** and the *n*-propylphenyliridium complex **3**, while the tube protected from light produced only **3**.

Further confirmation of the identity of the bis-phosphine complex **6** was achieved by its reactions with HBF_4. This product $(\eta^5\text{-}C_5Me_5)Ir(PMe_3)_2H^+BF_4^-$, which has been described previously.[11]

In analogy to the photochemical behavior of **2** irradiation of a benzene solution of syn/anti stereoisomers **8a** and **8b** with 6 equiv of PMe_3 produced as the major organometallic product **6** (93% yield, ferrocene internal standard) and free *trans*-butene mixed with a small amount of *cis*-butene (12:1).

Scheme VIII

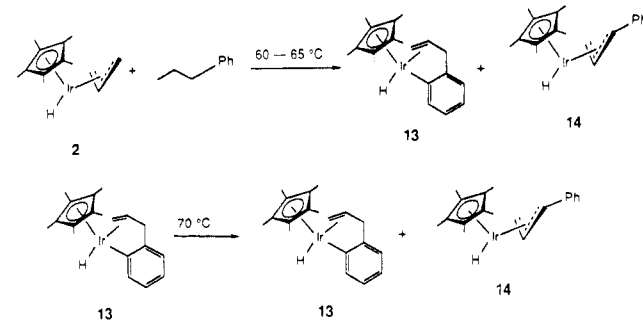

Scheme IX

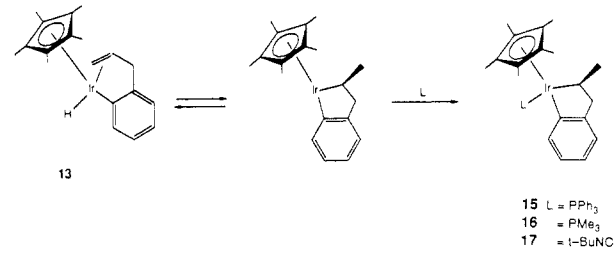

Thermolysis of 2 in *n*-Propylbenzene (Scheme VIII). Heating **2** in *n*-propylbenzene to 60–65 °C for 40 h led to the clean formation of two new organometallic complexes in a ratio of 4:1, each showing Ir–H resonances (δ −15.27 and −16.73, respectively). The major product, cyclometalated hydride **13**, was isolated in 44% yield by two crystallizations from pentane at −40 °C. Its ^1H NMR spectrum in C_6D_{12} shows five unique resonances for the η^2-allylic portion of the chelating ligand in the range of δ 3.25–2.4. In the ^{13}C NMR spectrum (C_6D_6) it shows resonances at δ 155.3 (s), 139.2 (s), 138.9 (d, J_{CH} = 153.5 Hz), 124.7 (dd, J_{CH} = 7.5, 154.4 Hz), 123.5 (dd, J_{CH} = 6.2, 151 Hz), 122.8 (dd, J_{CH} = 7.7, 157.2 Hz) for the aromatic carbons and δ 54.0 (d, J_{CH} = 153 Hz), 38.98 (t, J_{CH} = 125.3 Hz), and 27.8 (t, J_{CH} = 157.7 Hz) for the allylic carbons, consistent with the structure for **13** shown in Scheme VIII. In the solid-state IR spectrum the Ir–H stretch is seen at 2126 cm^{-1}. Curiously, irradiation of the hydride resonance in the ^1H NMR spectrum, centered at −15.53 ppm (C_6D_{12}), caused signals due to the two olefinic CH_2 protons at δ 2.55 and 2.44 to diminish substantially in intensity. We attribute this to spin saturation transfer. To gain more evidence for site exchange between the hydride ligand and the CH_2 olefinic hydrogens, variable-temperature ^1H NMR spectra were obtained. At 55 °C broadening of the resonances at δ 2.52, 2.44, and −15.53 occurred; however, temperatures high enough for complete coalescence could not be achieved. No exchange between the hydride hydrogen and any other hydrogen was observed. The minor product of the reaction above is assigned as $(\eta^5\text{-}C_5Me_5)Ir(syn\text{-}1\text{-phenyl-}C_3H_4)H$ (**14**), based on its ^1H and $^{13}C\{^1H\}$ NMR spectra (as a mixture with **13**).

Thermolysis of a C_6D_{12} solution of pure **13** at 70 °C for 18 h gave **13** and **14** in a ratio of 4:1, identical with the mixture obtained in the thermolysis reaction described above.

Addition of Dative Ligands (L = PMe_3, PPh_3, and *t*-BuNC) to 13 (Scheme IX). Addition of PPh_3, PMe_3, or *t*-BuNC to cyclometalated hydride **13** in benzene at room temperature resulted in the immediate formation of methyl-substituted iridacyclopentanes (**15**, L = PPh_3; **16**, L = PMe_3; and **17**, L = *t*-BuNC), respectively. In each case two stereoisomers of the iridacycles were produced in inequivalent amounts. The addition of PPh_3 produced the two stereoisomers of **15** in a ratio of 22:1. The major isomer was separated by crystallization from toluene/hexane and was fully characterized by standard spectroscopic techniques and microanalysis (see Experimental Section). In the reaction of **13** with PMe_3 the ratio of isomers produced was 8:1.

(10) (a) $CpCo(PMe_3)_2$: Juthani, B. Dissertation, Universitat Wurzburg, 1980. (b) $Cp^*Co(PMe_3)_2$: Werner, H.; Heiser, B.; Klingert, B.; Dolfel, J. *J. Organomet. Chem.* **1982**, *240*, 179. (c) $CpRh(PMe_3)_2$: Werner, H.; Feser, R.; Buchner, W. *Chem. Ber.* **1979**, *112*, 834. (d) $Cp^*Rh(PMe_3)_2$: Klingert, B.; Werner, H. *Chem. Ber.* **1983**, *116*, 1450. (e) $CpIr(PMe_3)_2$: Buchanan, J. M. Dissertation, University of California, 1985.

(11) Gilbert, T. M.; Bergman, R. G. *J. Am. Chem. Soc.* **1985**, *107*, 3502.

Scheme X

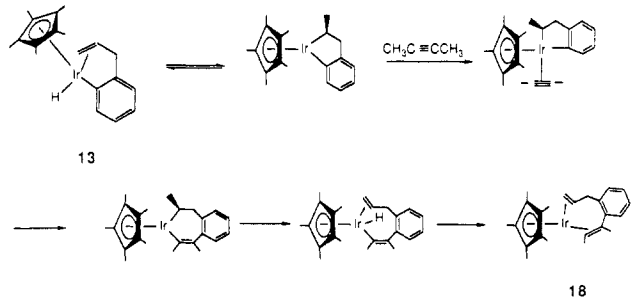

Scheme XI

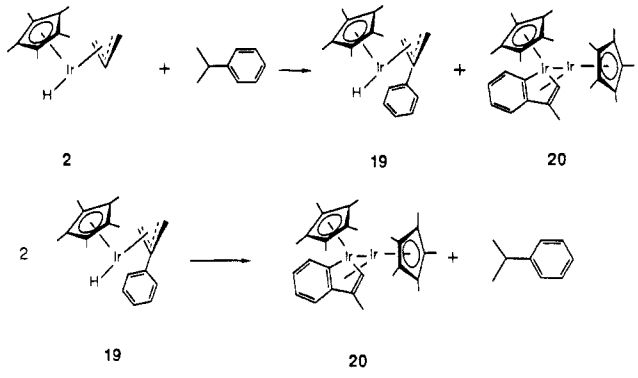

In this case the two complexes could not be separated from each other and were therefore characterized as a mixture (see Experimental Section). Addition of *t*-BuNC to **13** gave the two isomers of **17** in a ratio of 4.2:1. The major isomer could be obtained analytically pure by two crystallizations from pentane. The ^{1}H NMR (C_6D_6) of this isolated isomer showed resonances due to the metallacyclic system at δ 1.86 (d, J = 7 Hz, CH_3), 3.06 (t, J = 13.4 Hz, CH_2), 3.44–3.26 (m, CH and CH_2), 7.56–7.39 and 7.15–7.05 (m, aromatic). In the ^{13}C NMR (C_6D_6) spectra the metallacyclic carbons of **17** appear at δ 157.2 (s), 142.9 (s), 137.9 (dd, $^3J_{CH}$ = 6.7 Hz, J_{CH} = 153 Hz), 124.6 (dd, $^3J_{CH}$ = 7.5 Hz, J_{CH} = 154 Hz), 122.9 (dd, $^3J_{CH}$ = 7.7 Hz, J_{CH} = 155 Hz), 121.9 (br d, J_{CH} = 150 Hz), 53.4 (t, J_{CH} = 122 Hz), 26.9 (q, J_{CH} = 123.5 Hz), 12.0 (d, J_{CH} = 131 Hz). This complex gives a clean parent ion in the mass spectrum at m/e 529. Heating a C_6D_6 solution of this single isolated isomer of the *tert*-butyl isocyanide iridacycle **17** to 100 °C in either the presence or the absence of added *t*-BuNC did not produce any of the minor isomer, nor did it cause further transformations of **17**.

Addition of 2-Butyne to 13 (Scheme X). Heating a hexane solution of cyclometalated hydride **13** with added 2-butyne gave a single new organometallic product, **18**, isolated in 48% yield as clear crystals. Its ^{1}H NMR spectrum shows resonances for the aromatic protons at δ 7.3–7.2 and 7.1–7.0 (m) and for the η^2-allylic protons δ 3.81 (dd, J = 2.1, 16 Hz), 3.39 (dd, J = 3.6, 16 Hz), 2.76 (m), 1.56 (dd, J = 1.7, 8.2 Hz), and 0.64 (dd, J = 1.8, 10 Hz), while the unique olefinic proton on the η^2-vinylic group appears at δ 2.62 (q, J = 6.7 Hz). The methyl groups appear at δ 1.69 (d, J = 6.7 Hz) and 1.64. In the ^{13}C NMR spectrum the aromatic carbons are at δ 145.1 (s), 135.5 (s), 131.0 (dd, J = 6.6, 154.6 Hz), 128.6 (d, J = 152 Hz), 127.6 (dd, J = 7.6 Hz, obscured by solvent), and 125.3 (dd, J = 7.8, 158 Hz). The allylic carbons appear at δ 42.6 (d, J = 149 Hz), 35.3 (t, J = 126 Hz), and 27.8 (t, J = 154.3 Hz) while the olefinic carbons are at δ 37.6 (s) and 32.4 (d, J = 151 Hz). Inspection of the ^{1}H NMR spectrum of the crude reaction mixture showed no observable formation of the iridacycle expected in analogy to those isolated from the reactions between **13** and PMe_3, PPh_3, or *t*-BuNC.

Thermolysis of the Allyliridium Hydride 2 in Cumene (Isopropylbenzene) (Scheme XI). Heating a solution of allyl hydride **2** in cumene to 60–65 °C for 40 h gave a dark red solution. By ^{1}H NMR spectroscopy (C_6D_6) two major products had been produced. The ratio of products depends strongly on initial concentration and reaction time. From the crude reaction material, the 2-phenylallyl complex **19** was isolated by column chromatography as light yellow crystals in 16% yield and characterized by standard spectroscopic means, although the failure to separate it from ca. 5% of an unknown impurity precluded microanalysis. A second dark red complex was also isolated in 18% yield which, on the basis of its spectroscopic and analytical properties, was assigned structure **20** shown in Scheme XI. This unusual diridium complex was characterized by standard spectroscopic techniques, microanalysis, and single-crystal X-ray diffraction (vida infra). In the ^{1}H NMR (C_6D_6) spectrum, the methyl group signal appears as a singlet at δ 2.09, and the unique CH proton absorbs at δ 6.49. Of interest is the strong absorption at λ_{max} = 500 nm (ϵ = 1.5 × 10^3) in the UV–visible spectrum.

Heating a solution of the 2-phenylallyliridium hydride **19** in C_6D_{12} to 70 °C gave the dinuclear complex **20** and cumene in a one-to-one ratio.

Table I. Selected Bond Distances (Å) and Angles (deg) for complex **20**

intramolecular distances			intramolecular angles			
atom 1	atom 2	distance	atom 1	atom 2	atom 3	angle
Ir1	Ir2	2.749 (1)	Cp1	Ir1	Ir2	152.6
			Cp1	Ir1	C1	138.8
Ir1	C1	2.010 (6)	Cp1	Ir1	C8	139.7
Ir1	C8	1.998 (6)	C1	Ir1	C8	77.7 (3)
Ir1	C11	2.216 (6)	Cp2	Ir2	Ir1	141.4
Ir1	C12	2.175 (6)	Cp2	Ir2	C1	144.3
Ir1	C13	2.196 (6)	Cp2	Ir2	C6	142.4
Ir1	C14	2.251 (6)	Cp2	Ir2	C7	142.0
Ir1	C15	2.245 (7)	Cp2	Ir2	C8	147.0
Ir1	Cp1	1.864	C1	Ir2	C8	67.9 (2)
Ir2	C1	2.254 (6)	Ir1	C1	Ir2	80.1 (2)
Ir2	C6	2.200 (6)	Ir1	C8	Ir2	80.4 (2)
Ir2	C7	2.150 (6)				
Ir2	C8	2.249 (7)	Ir1	C1	C6	116.4 (5)
Ir2	(plane)	1.829	C1	C6	C7	112.8 (5)
			C6	C7	C8	111.8 (6)
Ir2	C21	2.165 (7)	C7	C8	Ir1	120.6 (5)
Ir2	C22	2.189 (7)	C8	Ir1	C1	77.7 (3)
Ir2	C23	2.186 (7)				
Ir2	C24	2.209 (7)	Ir1	C1	C2	127.6 (5)
Ir2	C25	2.187 (7)	C6	C1	C2	115.9 (5)
Ir2	Cp2	1.824	C1	C2	C3	123.5 (6)
			C2	C3	C4	120.1 (7)
C1	C2	1.406 (9)	C3	C4	C5	120.4 (7)
C2	C3	1.351 (9)	C4	C5	C6	121.2 (7)
C3	C4	1.407 (10)	C1	C6	C5	118.6 (6)
C4	C5	1.343 (10)	C5	C6	C7	128.5 (6)
C5	C6	1.435 (9)	C6	C7	C9	125.4 (6)
C1	C6	1.462 (8)	C8	C7	C9	122.5 (6)
C6	C7	1.425 (8)				
C7	C8	1.391 (9)				
C7	C9	1.509 (9)				

Scheme XII

Crystal and Molecular Structure of Iridium Dimer 20. Slow evaporation of diethyl ether from a diethyl ether/acetonitrile solution gave deep red crystals of **20**. The structure was solved in an X-ray diffraction study performed by Dr. F. J. Hollander; details are given in the Experimental Section. An ORTEP diagram is shown in Figure 1. Selected bond distances and angles are given in Table I. From this structure, complex **20** is best formulated as a diiridium complex with one metal center acting as a metallaindenyl ligand coordinated to the other iridium center.

Synthesis of (η^5-C_5Me_5)Ir(η^3-C_3H_5)R: R = c-C_6H_{11}, CH_3, $CH_2C_6H_5$, and C_6H_5 (21–24) (Scheme XII). Addition of cy-

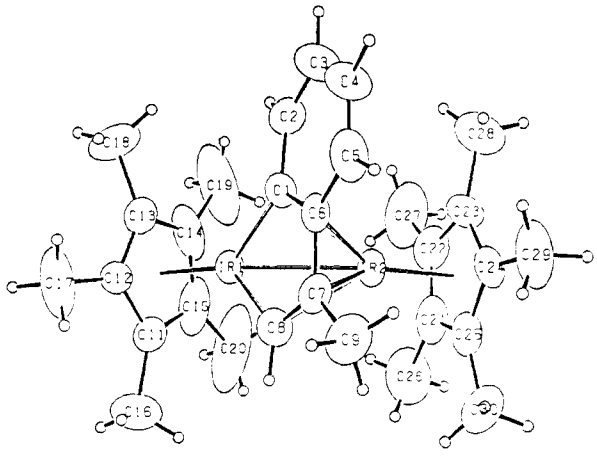

Figure 1. ORTEP diagram of complex **20**.

Scheme XIII

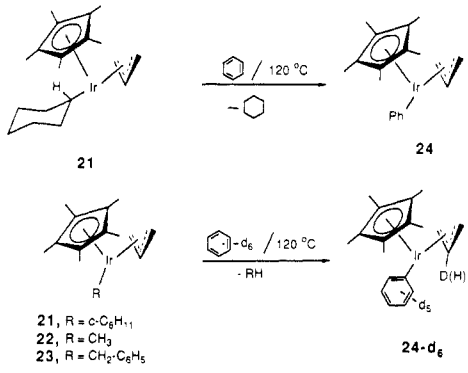

clohexylmagnesium chloride to the allyl chloride **1** in diethyl ether gave a 51% yield of clear, air-stable crystals of (η^5-C_5Me_5)Ir-(η^3-C_3H_5)(c-C_6H_{11}) (**21**). The cyclohexyl complex was characterized by standard spectroscopic and analytical techniques. In the ^{1}H NMR the π-allyl protons appear at δ 3.23 (m), 2.85 (d, J = 6.5 Hz), and 1.08 (d, J = 8.8 Hz). The cyclohexyl proton resonances were complex, therefore a COSY NMR spectrum was obtained; this spectrum in conjunction with a ^{1}H/^{13}C heteronuclear 2-D spectrum made assignments of the cyclohexyl proton resonances possible. From the 2-D spectral information the α-cyclohexyl proton can be unambiguously assigned to the proton resonance at δ 0.50 (t, J = 12.2 Hz) which contrasts with the lower field chemical shift observed for the α-cyclohexyl proton in (η^5-C_5Me_5)(PMe_3)Ir(H)(c-C_6H_{11}).[2a] In the ^{13}C NMR spectrum the allylic carbons appear at δ 69.4 (d, J = 160.2 Hz) and 37.1 (t, J = 156 Hz) while the cyclohexyl carbon resonances appear at δ 39.6 (t, J = 123.6 Hz), 32.7 (t, J = 122.5 Hz), 28.5 (t, J = 128 Hz), and 24.3 (d, J = 130 Hz). Complexes **22–24** were synthesized by similar procedures and displayed no unusual spectral features (See Experimental Section).

Thermolysis of Complexes 21–23 in Benzene (Scheme XIII). Thermolysis of the allylcyclohexyliridium complex **21** in C_6H_6 at 120 °C for 10 h gave the allyl phenyl complex **24** in 55% isolated yield. Heating solutions of **21–23** at various temperatures in C_6D_6 (see Experimental Section) cleanly produced the allylphenyl complex **24-d_6**—containing a deuterium atom in the central allylic position—along with the corresponding R–H species by ^{1}H NMR spectroscopy (Scheme XIII). With the methyl allyl and benzyl allyl complexes **22** and **23**, a small amount of the product contained hydrogen in the β-allylic position as determined by ^{1}H NMR spectroscopy. There was no exchange of deuterium into the starting materials during the course of the thermolysis reaction. Qualitatively the ease of reaction follows the order R = c-C_6H_{11} (**21**) > CH_2-C_6H_5 (**23**) > CH_3 (**22**). To test the reactivity of the allyl phenyl complex (**24**) it was heated in a C_6D_6 solution; temperatures up to 150 °C for 24 h produced no observable reaction by ^{1}H NMR spectroscopy.

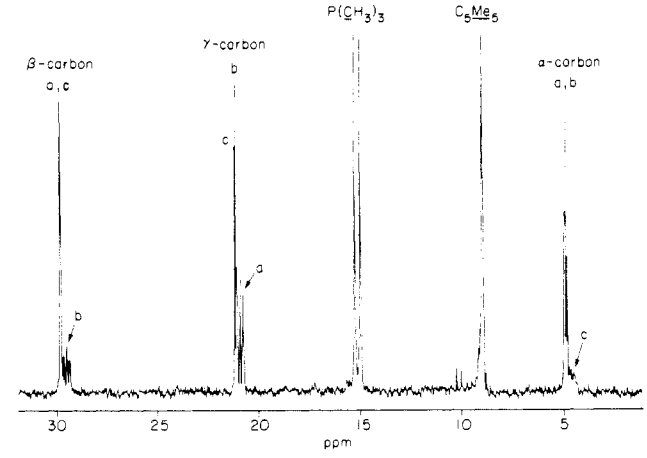

Figure 2. ^{13}C NMR spectrum (C_6D_6) of the alkyl region of **3-d_6**: (a) Ir-$CH_2CH_2CH_2D$, (b) Ir-CH_2CHDCH_3, (c) Ir-$CHDCH_2CH_3$.

Scheme XIV

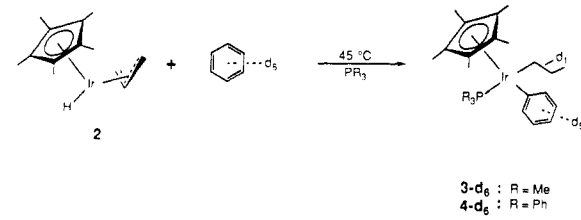

Mechanistic Studies

Reaction of 2 with C_6D_6 in the Presence of Phosphines (Scheme XIV). To gain information about the mechanism of addition of benzene to the (π-allyl)iridium hydride **2** (cf. Scheme II), the reaction was carried out in C_6D_6. A solution of **2** in C_6D_6 (ca. 0.01 M) containing 1.5 equiv of PMe_3 was heated to 45 °C for 16 h, giving **3-d_6** in 62% yield as clear crystals. The extent of deuteriation in the final product was determined by mass spectroscopy. The parent cluster for the complex matched the computer simulation for $C_{22}H_{30}D_6IrP^{\bullet+}$. This information suggests that only those deuterium atoms from a single C_6D_6 molecule are present in the final product. Additionally, in the mass spectrum of **3-d_6**, the major fragment corresponds to $M^+ - C_3H_6D$, suggesting that only one deuterium is located in the *n*-propyl group. By ^{1}H NMR spectroscopy (C_6D_6) there are no observable resonances for the aryl group in **3-d_6**; however, the complexity of the *n*-propyl group in the ^{1}H NMR spectrum precludes any compositional analysis of this ligand. From the ^{2}H{^{1}H} NMR spectrum (C_6H_6) it is clear that the arene substituent is completely deuteriated and that the single deuterium in the *n*-propyl group is distributed approximately equally in each of the α-, β-, and γ-positions. The alkyl region of the ^{13}C{^{1}H} NMR spectrum of **3-d_6** (Figure 2) also supports the scrambling of the deuterium into each position of the *n*-propyl group. Analogous results were obtained when C_6D_6 was utilized in the reaction with added PPh_3; **4-d_6** was isolated in 58% yield.

Kinetic and Isotope Effect Studies: Rate of Reaction of 2 with C_6R_6 (R = H and D) in the Presence of Phosphines. The rate of disappearance of the (π-allyl)iridium hydride **2** in C_6D_6 solvent was first determined for several different concentrations of PPh_3 (0.03–0.53 M). The rate was monitored through at least 3 half-lives by ^{1}H NMR spectroscopy with ferrocene as an internal standard. In all cases clean first-order rate constants were obtained. The rate was also determined at two different concentrations of PMe_3 (0.173 and 0.40 M). The values obtained from these studies are given in Table II. The rate is essentially independent of phosphine concentration.

With use of a constant concentration of PPh_3, the concentration of C_6H_6 was varied. This was achieved by using per deuteriocyclohexane (C_6D_{12}) as a diluent. The use of C_6D_{12} did not alter the products of the reaction under the conditions utilized here; however, use of C_6H_6/C_6D_{12} mixtures below 1 M C_6H_6 did give

Table II. Rate of Reaction of **2** with C_6D_6 and PR_3: Dependence on $[PR_3]$[a]

	$[PR_3] \times 10^2$	$k_{obsd} \times 10^5$
R = Ph	3	6.2
	7.6	7.25
	8.3	7.1
	28.5	7.0
	53	7.3
R = Me	17.3	7.5
	40	7.5

[a] In C_6D_6 at 45 °C.

Table III. Rate of Reaction of Allyl Hydride **2** with C_6R_6 in the Presence of PPh_3[a]

	$[C_6R_6]$ (M)	$1/[C_6R_6]$	$k_{obsd} \times 10^5$ (s^{-1})	$1/k_{obsd} \times 10^{-4}$
R = H	1	1	2.6	3.85
	1.33	0.75	3.0	3.33
	2	0.5	4.0	2.50
	4	0.25	5.6	1.79
R = D	1.33	0.75	2.7	3.70
	2	0.5	3.5	2.82
	3	0.33	4.3	2.33
	4	0.25	5.2	1.92
	11.3	0.088	7.1	1.41

[a] In C_6D_{12} at 45 °C.

Scheme XV

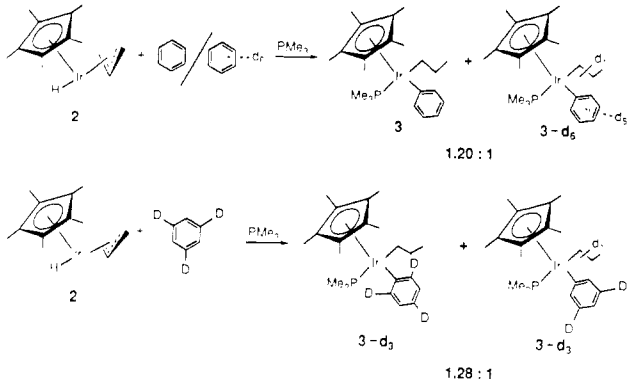

rise to side products. The results obtained at four different concentrations of C_6H_6 (1–4 M) are given in Table III; these show that the rate is dependent on the concentration of C_6H_6. A plot of k_{obsd} versus $[C_6H_6]$ is shown in Figure 3a, and a plot of $1/k_{obsd}$ versus $1/[C_6H_6]$ is shown in Figure 3b. The linearity of the plot in Figure 3b is consistent with a mechanism in which the starting material **2** undergoes equilibration with a transient intermediate X (eq 4), followed by reaction of X with benzene (eq 5). This gives the rate law shown in eq 6. At high benzene concentrations, pseudo-first-order kinetics are observed, allowing measurement of the benzene-concentration-dependent rate constant k_{obsd}. From the intercept of the plot in Figure 3b, $k_1 = 9.1 \times 10^{-5}$, and from

$$\mathbf{2} \underset{k_{-1}}{\overset{k_1}{\rightleftharpoons}} \mathrm{X} \qquad (4)$$

$$\mathrm{X} + C_6R_6 \xrightarrow{k_2} \text{products} \qquad (5)$$

$$\text{rate} = -\frac{d[\mathbf{2}]}{dt} = \frac{k_1k_2[C_6R_6]}{k_{-1} + k_2[C_6R_6]}[\mathbf{2}] = k_{obsd}[\mathbf{2}] \qquad (6)$$

the slope, $k_{-1}/k_2 = 2.62$. With use of a constant concentration of PPh_3, the concentration of C_6D_6 was varied, again with C_6D_{12} as the diluent. A plot of $1/k_{obsd}$ versus $1/[C_6D_6]$ is shown in Figure 3b. From this plot $k_1 = 9 \times 10^{-5}$ and $k_{-1}/k_2 = 3.1$. From the studies involving C_6H_6 and C_6D_6, $k_H/k_D = 1.24$ for k_2.

Competition between C–H and C–D Bonds in Benzene (Scheme XV). In order to explore the effect of deuteriation on the product-forming steps of the reaction a solution of the π-allyl hydride **2** in a 1:1 mixture of C_6D_6/C_6H_6 containing 1.5 equiv of PMe_3 was heated to 45 °C for 14 h followed by the removal of volatile materials. Integration of the ortho-aromatic protons versus the bound PMe_3 hydrogens in the crude reaction product gave a ratio of 1.20 ± 0.02 for **3**/**3-*d*$_6$**. This is the intermolecular k_H/k_D (isotope effect) for reaction of the intermediate with benzene.

In order to compare this value with the corresponding intramolecular isotope effect, a solution of **2** in 1,3,5-$C_6D_3H_3$ containing 1.5 equiv of PMe_3 was then heated to 45 °C for 14 h. The volatile materials were removed and a ^1H NMR spectrum (THF-d_8) was obtained. Integration of the *m*- versus *o*-aryl protons gave a ratio of (1:28 ± 0.04):1, which is the relative amount of the two isomers of **3-*d*$_3$** shown in the second line of Scheme XV.

Reaction of 2 with C_6D_6 in the Absence of L (Scheme XVI). Heating a solution of the (π-allyl)iridium hydride **2** in C_6D_6 (ca. 0.01 M) to 45 °C for 24 h with no added phosphine led to gradual darkening of the solution. Removal of the volatile materials gave a brown solid which after sublimation gave 46–60% yields of a white, air-sensitive solid. A ^1H NMR spectrum (C_6D_6) showed only a single resonance at δ 1.84 while in the $^2H\{^1H\}$ NMR spectrum (C_6H_6) resonances at δ 2.93, 2.49, 2.17, and −16.6 were observed. A solid-state IR spectrum showed a strong Ir–D stretch at 1513 cm^{-1} ($\nu_{Ir-H}/\nu_{Ir-D} = 1.385$), and in the mass spectrum a parent ion was observed at m/e 376. From the above evidence the product of the reaction can be identified as (η^5-C_5Me_5)Ir-(η^3-C_3D_5)D (**2-*d*$_6$**), the product of proton/deuterium exchange. There is no evidence for incorporation of deuterium into the η^5-C_5Me_5 ligand. There is no apparent reaction when a dilute solution of **2** in C_6H_6 is heated to 45 °C.[12]

Kinetics of Reaction between 2-*d*$_6$, C_6D_6, and PPh_3. The availability of **2-*d*$_6$** allowed us to examine the rate of reaction between it and C_6D_6 in the presence of PPh_3. Measurements were made at several concentrations of C_6D_6 in C_6D_{12} (Table IV). A plot of $1/k_{obsd}$ versus $1/[C_6D_6]$ is given in Figure 3b. The linearity of this plot is again consistent with the reversible formation of a transient intermediate, leading to a rate law of the form given in eq 6. From this plot $k_1 = 1.10 \times 10^{-4}$ and $k_{-1}/k_2 = 1.8$. These data along with those obtained from the reaction between **2** and C_6D_6 (with PPh_3) give k_H/k_D for $k_1 = 0.81$ and (assuming k_2 does

Scheme XVI

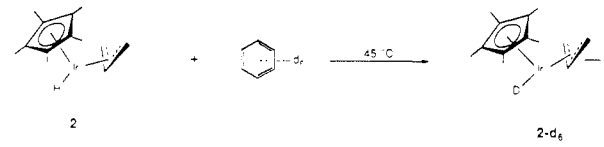

Scheme XVII

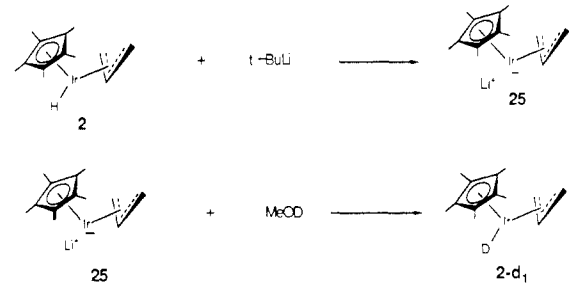

Table IV. Rate of Conversion of **2-*d*$_6$** to **3-*d*$_{12}$**[a]

$[C_6D_6]$ (M)	$1/[C_6D_6]$	$k_{obsd} \times 10^5$	$1/k_{obsd} \times 10^{-4}$
1	1	4.0	2.48
2	0.5	5.8	1.73
3	0.33	6.5	1.54
4	0.25	7.4	1.35
11.3	0.088	10.9	0.92

[a] In C_6D_{12} at 45 °C.

(12) The use of high concentrations of **2** in C_6H_6 at 45 °C leads to (η^5-C_5Me_5)(Ph)Ir(η^1,η^3-C_3H_4)(μ-H)Ir(η^5-C_5Me_5): McGhee, W. D.; Bergman, R. G., manuscript in preparation.

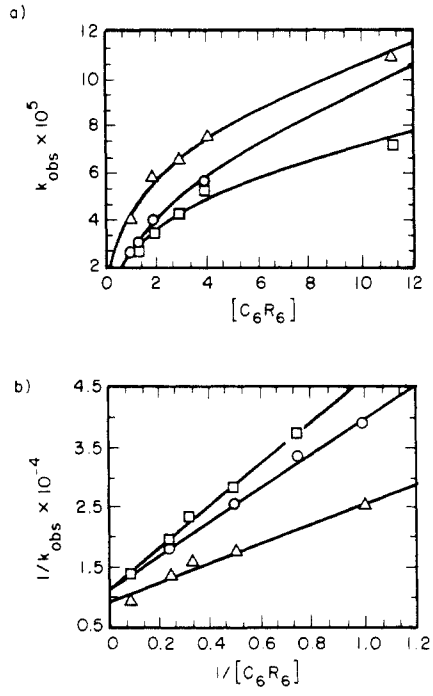

Figure 3. (a) Plot of observed rate constants versus benzene concentration: (○) reaction between **2** and C_6H_6, (□) **2** and C_6D_6, (△) **2**-d_6 and C_6D_6. (b) Inverse plot: symbols denote the same reactions as in plot **5a**.

Scheme XVIII

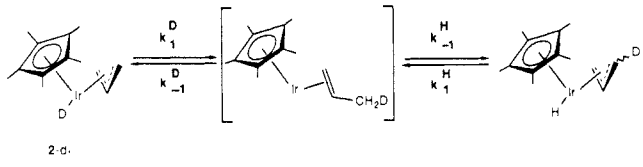

Scheme XIX

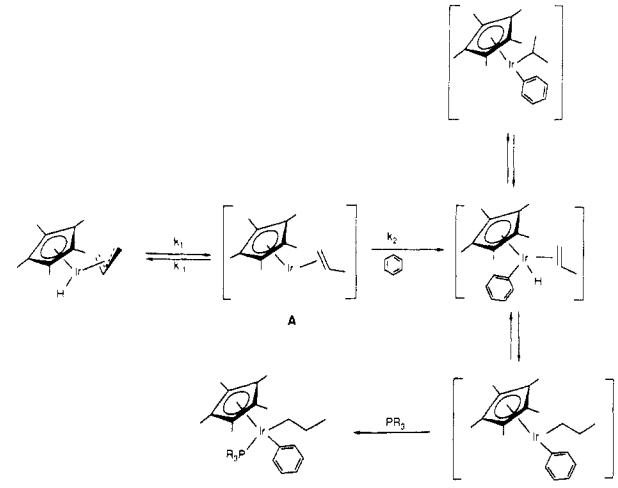

Scheme XX

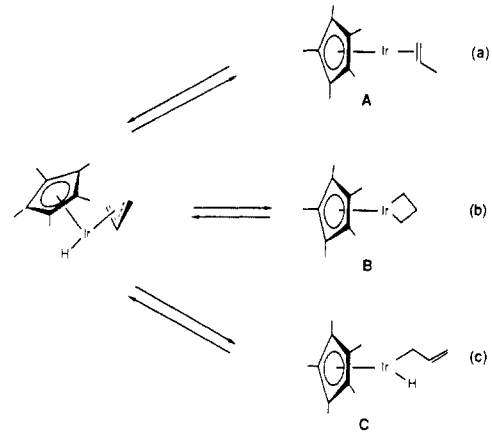

not change upon replacement of **2** with **2**-d_6) k_H/k_D for k_{-1} = 1.72. The product of this reaction was determined to be (η^5-C_5Me_5)Ir(PMe_3)(C_6D_5)C_3D_7 by ^1H, $^{31}P\{^1H\}$ NMR and mass spectrometry.

Deprotonation of the (π-Allyl)iridium Hydride 2 and the Synthesis of (π-Allyl)iridium Deuteride 2-d_1 (Scheme XVII). Addition of *t*-BuLi to a solution of **2** in pentane at room temperature gave a green solid in 74% yield identified as (η^5-C_5Me_5)Ir(η^3-C_3H_5)$^-$Li$^+$ (**25**) on the basis of its ^1H and $^{13}C\{^1H\}$ NMR spectra and elemental analysis. This anionic complex is extremely air sensitive, but it can be kept indefinitely at −40 °C in the drybox. Solutions of **25** in THF-d_8 slowly darken at room temperature under nitrogen.

Addition of an excess of MeOD to a pentane slurry of **25** gave (η^5-C_5Me_5)Ir(η^3-C_3H_5)D as a light brown solid in 81% isolated yield. By $^2H\{^1H\}$ NMR spectroscopy the (η^3-C_3H_5) portion of the complex has not undergone any deuteriation (>95% protons). This is also supported by the ^1H NMR spectrum (C_6D_6). Of particular note in the ^1H NMR spectrum is the loss of observable coupling between the α-allyl protons and the hydride. The extent of deuteriation at the Ir–D position is >95% as analyzed by ^1H and $^2H\{^1H\}$ NMR and solid-state IR spectroscopy. In the IR spectrum the Ir–D absorption appears at 1514 cm^{-1} (ν_{Ir-H}/ν_{Ir-D} = 1.384).

Deuterium Scrambling Observed on Thermolysis of the Allyliridium Deuteride 2-d_1 (Scheme XVIII). A C_6D_{12} solution of **2**-d_1 in a sealed NMR tube was heated to 45 °C and the reaction monitored by ^1H NMR spectroscopy. The appearance of a singlet at δ- 16.7 was observed as well as changes in the π-allyl protons. After 5 h the solvent was removed in vacuo and replaced with C_6H_6. By $^2H\{^1H\}$ NMR spectroscopy, resonances of approximately equal intensity at δ 2.51 and 2.21 had appeared, corresponding to deuteriation of the α-allylic positions. The β-allylic position did not undergo exchange to any observable extent (<5%). After the solution was heated to 45 °C for 17.5 h $^2H\{^1H\}$ NMR analysis showed no new resonances. By integration of the α-allylic versus the Ir–D resonances a value for K_{eq} of 2.2 ± 0.14 (after correction for the 4:1 statistical preference for the terminal allylic positions) was calculated for the process illustrated in Scheme XVIII.

Discussion

Reaction of the (π-Allyl)iridium Hydride 2 with Benzene. The addition of PMe_3 to **2** was initially investigated to determine whether the π-allyl ligand could be converted from a four electron to a two electron donating σ-allyl group. Surprisingly, we observed the major product from **2** to be the *n*-propylphenyliridium complex **3**, formed by oxidative addition of the C–H bond of the solvent benzene, followed by migration of H to the C_3 fragment and addition of phosphine (Scheme II). Overall, the reaction of **2** with benzene results in conversion of the π-allyl ligand to a saturated *n*-propyl group by accepting a hydrogen from both iridium and benzene. A mechanism that is consistent with the evidence presented for this reaction is shown in Scheme XIX.

The role of benzene in the rate law for this reaction was established by determining the changes in the observed rate of reaction as a function of benzene concentration. As shown in parts a and b of Figure 3, changing the concentration of benzene clearly affected the rate of reaction. The simplest mechanism that fits the rate data (Scheme XIX) involves reversible formation of an intermediate (e.g., A) from **2** which is then competitively trapped by benzene. From this proposed path the rate law given in eq 6 can be derived, and k_1 (the rate of formation of the intermediate from **2**), as well as the partitioning rate constant ratio k_{-1}/k_2, can be determined.

The η^2-propene complex A illustrated in Scheme XIX is not the only possible structure for the intermediate formed reversibly from **2**. Along with A, two other possibilities are shown in Scheme XX. Formation of A involves migration of the hydride to the α-position of the allyl ligand. A second possibility postulates

Scheme XXI

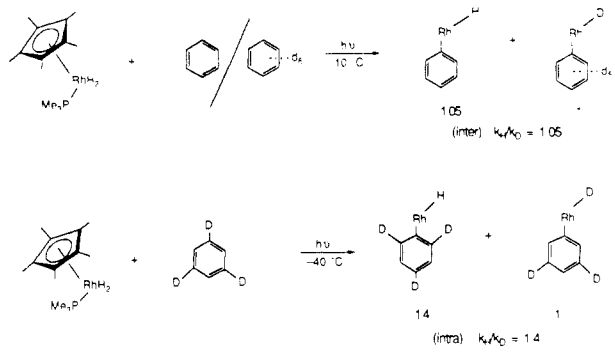

Scheme XXII

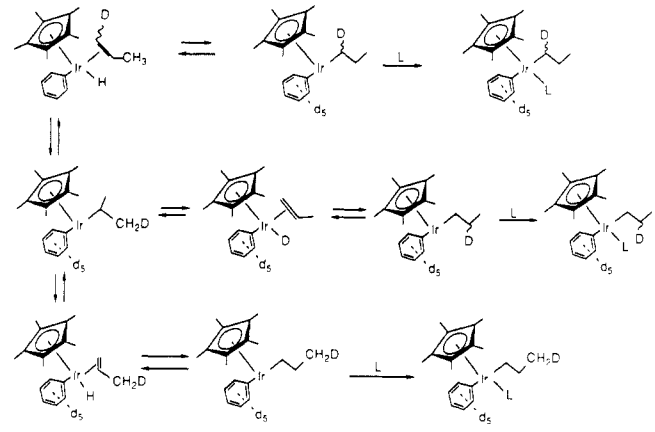

reversible formation of a 16-electron iridacyclobutane (B), resulting from migration of the hydride to the β-position of the π-allyl ligand. The third pathway involves η^3- to η^1-allyl conversion leading to C.[13]

To determine if migration takes place reversibly to the α- and/or β-allylic positions, isotopic substitution at the hydride position was needed. However, addition of $LiBEt_3D$ to the chloride **1** gave **2-d_1** with deuterium located in both the hydride and β-allylic positions. Because regiospecific synthesis of **2-d_1** could not be achieved by direct addition of $LiBEt_3D$ to **1**, an alternate route was sought. We previously used *t*-BuLi to deprotonate an iridium hydride; therefore, we used this method for removing the hydride in **2** leading to **25** (Scheme XVIII).[11] Quenching the resulting anion with MeOD selectively placed deuterium at iridium in **2-d_1** with no observable scrambling. Subsequent thermolysis of **2-d_1** gave scrambling only into the α-allylic positions, supporting our initial postulate of intermediate A in Scheme XIX. This experiment also shows that either reversible migration to the β-allylic position does not take place or this process is stereospecific, giving no isotope exchange. Because other well-documented cases of migration of metal hydrides to the α-position in α-allyl complexes are known, we feel that this is the most likely route for the scrambling process.

To gain additional information about the nature of the intermediate, isotope effect studies were carried out. First, the isotope effect on the reaction of the intermediate with benzene was examined. By utilizing C_6D_6 in place of C_6H_6, and measuring the rate of the reaction at varying concentrations of this in the inert solvent C_6D_{12}, the second reciprocal plot in Figure 3b (analogous to the one obtained with ordinary benzene) was obtained. From these two reciprocal plots, values for k_1 and k_{-1}/k_2 in Scheme XIX for reaction with protonated and deuteriated benzene were obtained. In the suggested mechanism the initial k_1 and k_{-1} steps do not involve benzene. Their values, therefore, should not be affected by this isotopic perturbation. This was confirmed for k_1, where values of 9.0 and 9.1 $\times 10^{-5}$ were obtained with C_6H_6 and C_6D_6, respectively. By making this reasonable assumption also for k_{-1}, the measured k_{-1}/k_2 values can be used to calculate the isotope effect in the k_2 step; this value turns out to be 1.24. As an independent check of this result, a direct competition experiment using a mixture of C_6H_6 and C_6D_6 was carried out and a k_H/k_D value of 1.20 was obtained by NMR analysis (Scheme XV). this is in good agreement with the calculation from direct rate data.

The presence of an isotope effect confirms the involvement of benzene in the k_2 step of the reaction. Its modest magnitude suggests that formation of an η^2-arene complex may intervene between the first intermediate and the C–H activation step in our reaction. In a study of the mechanism of C–H activation of benzene by rhodium,[14] Jones and Feher also observed a small primary isotope effect. However, in addition they applied the method of comparative intra- and intermolecular isotope effects developed earlier by Dolbier and his co-workers in the investigation of several organic thermal rearrangement reactions.[15] The Jones/Feher system is illustrated in Scheme XXI along with their experimentally derived k_H/k_D values. Significantly, they found substantially different k_H/k_D values in the (intermolecular) competition of Cp*(L)Rh(L = PMe_3) for hydrogen and deuterium in *separate* molecules (C_6D_6 versus C_6H_6), compared with (intramolecular) competition of the intermediate for hydrogen and deuterium in the *same* molecule (the H and D atoms in 1,3,5-$D_6D_3H_3$). These results require the intervention of an intermediate between Cp*(L)Rh and the insertion product. Jones and Feher postulated an η^2-arene complex as this intermediate.

Following the example of Jones and Feher, we decided to measure the intramolecular isotope effect in our system using 1,3,5-$C_6D_3H_3$, so that it could be compared with the intermolecular C_6D_6 versus C_6H_6 isotope effect discussed above. From NMR analysis of this 1.28 ± 0.04 was obtained for the intramolecular k_H/k_D (Scheme XV). Thus there seems to be a difference between the two measurements, but the magnitude of the difference is considerably smaller than it is in the Cp*(L)Rh case. Because of this, we cannot decide definitively whether the intermediate formed from **2** inserts into benzene C–H bonds directly or forms a second intermediate (e.g., an η^2-complex) before this insertion step occurs. However, the intervention of such a complex provides a reasonable way to account for the small magnitude of the overall isotope effect in our system.

Having determined the isotope effect on the k_2 step, a similar study was carried out on the k_1, k_{-1} step by deuteriating the starting complex. Thus, the rate of reaction of **2-d_6** with varying concentrations of C_6D_6 was measured (see Figure 3, a and b). By making the reasonable assumption that k_2 does not change upon replacement of **2** with **2-d_6**, values of 0.81 and 1.72 were obtained for k_H/k_D in k_1 and k_{-1}, respectively. As an independent check on these measurements we determined the equilibrium isotope effect K_{eq} for the reversible scrambling in **2-d_1**. This equilibrium effect was found to be 2.2 ± 0.14 (Scheme XVIII). This is in reasonable agreement with K_{eq} calculated from the isotope effects in k_1 and k_{-1} (i.e., $K_{eq} = (k_{-1}^H/k_{-1}^D)(k_1^D/k_1^H) = (1.72)(1/0.81) = 2.1$).

The magnitude of the kinetic isotope effect on k_1 is consistent with those measured in other related reductive elimination reactions at iridium and rhodium.[14,16] For example, in arene elimination from $(\eta^5\text{-}C_5Me_5)Rh(PMe_3)(3,5\text{-}C_6H_3Me_2)H$, $k_H/k_D = 0.51$; inverse isotope effects of slightly smaller magnitude have also been observed in the reductive elimination of alkanes from $(\eta^5\text{-}C_5Me_5)Ir(PMe_3)(R)H$ and $(\eta^5\text{-}C_5Me_5)(PMe_3)Rh(R)(H)$.[2a,b,14] These effects result from the conversion of a normal mode in the starting complex associated with the low-frequency metal hydride vibration to a normal mode in the transition state containing substantial higher-frequency C–H character associated with the

(13) For a recent discussion of η^3-to-η^1-allyl interconversion, see: Erker, G.; Berg, K.; Angermund, K.; Kruger, C. *Organometallics* **1987**, *6*, 2620.
(14) Jones, W. D.; Feher, F. J. *J. Am. Chem. Soc.* **1986**, *108*, 4814.
(15) (a) Dolbier, W. R.; Dai, S.-H. *J. Am. Chem. Soc.* **1972**, *94*, 3946. (b) Dolbier, W. R.; Dai, S.-H. *Ibid.* **1968**, *90*, 5028.
(16) (a) Buchanan, J. M.; Stryker, J. M.; Bergman, R. G. *J. Am. Chem. Soc.* **1986**, *108*, 1537.

Scheme XXIII

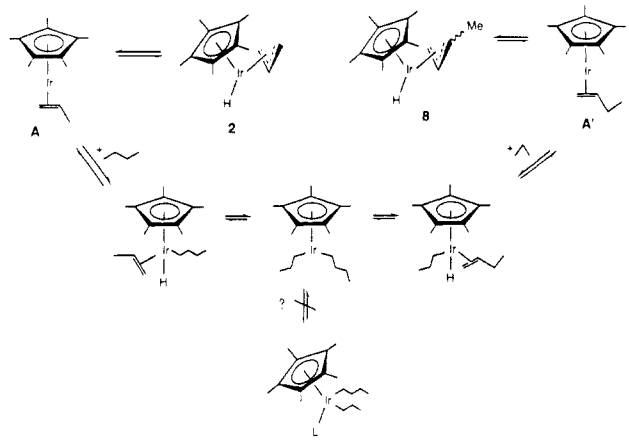

developing C–H bond in the newly forming propene ligand.

Upon C–H bond insertion, evidence for subsequent reversible hydride migration to the η^2-propene ligand prior to trapping is provided by the isotope distribution in the final product **3-d_6** when C_6D_6 is used. The observation that deuterium is located in all positions in the *n*-propyl group can be explained by rapid insertion/de-insertion into either the CH_2 or CH portion of the propene ligand as shown in Scheme XXII. Because only six deuterium atoms are incorporated into the final product it is required that the benzene does not reductively eliminate after olefin–hydride insertion takes place. The trapping of the hydride insertion product by phosphine was shown to occur in a rapid irreversible step as shown by the kinetic data and the stability of the final product, **3**. The trapping of only the linear *n*-propyl rather than the bulkier isopropyl substituted intermediate emphasizes the sensitivity of this system to steric effects.

Because the rate of conversion of **2** to **3** and **4** is independent of the nature and concentration of phosphine, PR_3 must react with the manifold of phenyl-containing intermediates in Scheme XIX much faster than they eliminate benzene to return to **A**. In the absence of phosphine, however, the deuterium exchange experiment illustrated in Scheme XVI demonstrates that this slower process has an opportunity to occur.

Reaction of the (π-Allyl)iridium Hydride 2 with *n*-Butane and Isobutane. Having demonstrated that allyl hydride **2** is reactive toward the C–H bonds of C_6H_6 and cyclopropane, we wished to explore its interaction with less reactive saturated hydrocarbons. Thermolysis of **2** with *n*-butane in the presence of PMe_3 did not give the expected *n*-propyl-*n*-butyliridium complex, in analogy to the benzene and cyclopropane reactions. However, the linear alkane did react, leading to the (η^3-1-methallyl)iridium complexes **8a** and **8b** shown in Scheme IV in both the presence and absence of phosphine. Similar behavior was observed with the branched alkane isobutane, leading to 2-methallyl complex **9**. These products arise from replacement of the parent allyl ligand in **1** by a substituted allyl ligand formed by dehydrogenation of the alkane solvent. The original π-allyl group again serves as a hydrogen acceptor, but the overall course of this reaction is modified by the presence of hydrogens on the entering carbon fragment that are capable of β-elimination. Analogous metal-mediated hydrogen-transfer reactions between alkanes and alkenes have been reported by Crabtree and Felkin and their co-workers.[2g,h]

We presume that in these reactions an overall equilibration is taking place that interconverts the methyl-substituted and unsubstituted allyl complexes with the corresponding alkanes; the large excess of alkane solvent *n*-butane drives the reaction completely toward the 1-methallyl side of the equilibrium. As shown in Scheme XXIII, it seems most likely that this process proceeds via intermediates identical or analogous with those postulated in the benzene and cyclopropane reactions. Thus, we assume that **2** once again forms small amounts of η^2-propene complex **A**, similarly, **8** equilibrates with corresponding butene complexes such as **A'**. The sequence of C–H oxidative addition and migratory insertion steps shown in the scheme then equilibrates these two species with the (alkene)(alkyl)(hydride) intermediates shown, and presumably with (η^5-C_5Me_5)Ir(*n*-butyl)(*n*-propyl). We do not know why this 16-electron dialkyl complex is not trapped by PMe_3 to give stable (η^5-C_5Me_5)(PMe_3)Ir(*n*-butyl)(*n*-propyl). We have not been able to prepare this material to test its stability to the reaction conditions.

Having obtained methallyliridium complexes from these reactions, we explored their reactions with benzene and PMe_3. In analogy to our observations with the parent allyl hydride, the methallyliridium hydride isomers were converted to their corresponding (η^5-C_5Me_5)Ir(PMe_3)(phenyl)(R) (R = *n*-butyl and isobutyl) complexes (Scheme VI). This establishes an overall sequence in which (π-allyl)iridium hydride **2** and either *n*-butane or isobutane is first converted to **8a**, **8b**, and **9**, respectively, followed by reaction with benzene to give **11** and **12**. This sequence is a rare example of the sequential C–H activation of two different hydrocarbons at one metal center.

Reaction of π-Allyl Hydride 2 with *n*-Propyl- and Isopropylbenzene. Having explored the reactivity of **2** with aromatic and saturated hydrocarbons, we decided to complete this study by examining the reactivity of the allyl hydride with organic compounds having sp^3 and sp^2 hydrogens in the same molecule. As shown in Scheme VIII, the observation of 1-phenylallyliridium hydride **14** in the reaction mixture from the thermolysis of **2** in *n*-propylbenzene demonstrated that at least to some extent **2** will activate the saturated alkyl group in the presence of a phenyl substituent. However, the major product of this reaction is **13**, which is the result of both alkyl and aromatic C–H activation. Furthermore, **13** and **14** are interconvertible. This was demonstrated by isolation of pure **13**, followed by its thermal conversion to a 4:1 equilibrium mixture of the two products.

Complex **13** undergoes a dynamic hydrogen-scrambling process that can be detected by NMR spectrometry. The NMR observations can be accounted for by postulating rapid insertion/de-insertion of the olefinic portion of the unusual η^1,η^2-CH_2=$CHCH_2$-C_6H_4 ligand into the Ir–H bond. The NMR data indicate that the insertion process is regiospecific, giving only the 16-electron metallacyclic intermediate resulting from addition of the metal-bound hydrogen to the terminal CH_2 position. Confirmation of the operation of this reversible alkene insertion/deinsertion process is provided by trapping the proposed intermediate by addition of PPh_3, PMe_3, or *t*-BuNC, leading to adducts of structure **15–17** (Scheme IX). The two possible stereoisomers of each trapping product were observed in inequivalent amounts, but only one regioisomer is formed in each case. It appears that the ratio of stereoisomers is dependent on the size of the trapping ligand, the larger PPh_3 ligand giving predominately one isomer while the smaller *t*-BuNC gives significant amounts of both isomers.

The addition of 2-butyne to **13**, however, did not produce a product analogous to those observed above. The product of the reaction is assigned the structure **18** shown in Scheme X; the stereochemistry of the vinyl group in complex **18** was not unambiguously determined. This product might be formed by direct insertion of 2-butyne into the Ir–H bond, generating a vinyl iridium species. However, an intriguing alternative is suggested by the reaction of **13** with dative ligands. It seems likely that the iridacycle postulated in Scheme IX is formed here as well, but the alkyne-coordinated product is not stable; instead it undergoes insertion, β-elimination, and reductive elimination, as shown in Scheme X, leading to **18**. We are grateful to a referee for suggesting this mechanism.

In the reaction between allyl hydride **2** and cumene (isopropylbenzene), we were also able to detect the expected dehydrogenation product, 2-phenylallyliridium hydride **19**. However, as shown in Scheme XI we again isolated an unexpected product, dinuclear iridium complex **20**. In this case the ratio of products depended greatly on the reaction conditions. Longer reaction times, as well as the use of more concentrated solutions of **2**, favored the formation of **20**. Upon thermolysis, (π-phenyl)allyliridium hydride **19** led to a 1:1 mixture of cumene and dinuclear complex **20**. This result suggests that reaction between the parent (π-allyl)iridium hydride **2** and cumene leads initially (and se-

Scheme XXIV

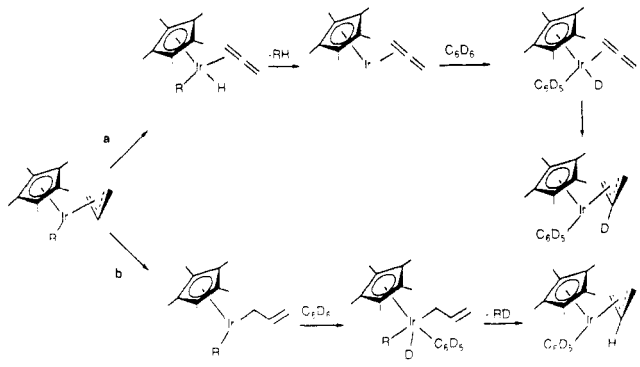

lectively) to dehydrogenation product **19**. This material is the source of dinuclear complex **20** in a secondary reaction. Complex **20** is similar to other reported bimetallic systems containing an η^5-metallacyclopentadienyl ligand.[17]

Thermolysis of Allylalkyliridium Complexes 21–23. The proposed migration of the hydride ligand in **2** to the π-allyl group, generating the π-propene intermediate **A**, led us to investigate whether alkyl groups would display similar reactivity; therefore, complexes **21–23** were synthesized. Some precedent for such migrations has appeared.[18] However, we observed instead reaction with the solvent benzene, giving exclusively exchange of the alkyl group for a phenyl group. A possible explanation for the isotopic distribution in the products from thermolysis in C_6D_6, involving π-allene complexes formed by β-elimination of the center hydrogen of the allyl group, is shown in Scheme XXIV. From the labeling studies it is apparent that the course of reaction favors pathway a. It is interesting that the iridium center avoids conversion to the Ir(V) state, via pathway b.

Conclusions. If we are correct in identifying the intermediate formed reversibly from **2** as the π-propene complex **A** illustrated in Schemes XIX and XX, **A** must have unusual properties. Of particular note is the comparison of this 16-electron intermediate with the 16-electron $Cp^*Ir(PMe_3)$ fragment previously demonstrated to insert readily into the C–H bonds of both alkanes and alkenes.[2b,16] $Cp^*Ir(PMe_3)$ undergoes *no* intramolecular insertion, but it reacts intermolecularly (almost undoubtedly with very low activation energy) with primary, secondary, and vinyl C–H bonds. The most rapid reaction of $Cp^*Ir(\eta^2$-propene) involves intramolecular insertion into the propene ligand, but this transformation is quite selective—reversible insertion into the allylic C–H bonds occurs rapidly and repeatedly under our reaction conditions, with (once again) no detectable product formed from intramolecular vinyl C–H insertion. Also, although the unsaturated propene complex **A** does undergo *intermolecular* insertion into the C–H bonds of benzene and *n*-alkanes, unlike $Cp^*Ir(PMe_3)$ it does not react readily with cyclohexane.

These differences in selectivity are perplexing, and we do not understand them fully. The facile and general intermolecular reactivity of $(\eta^5$-$C_5Me_5)(PMe_3)Ir$ can be rationalized by the high basicity of the Ir center, and the relatively small size of the PMe_3 ligand, allowing even sterically bulky substrates such as cyclohexane to approach the metal. Replacing the PMe_3 group with a CO ligand makes the metal center less electron rich, but also more sterically accessible, and so intermolecular C–H activation can still proceed.[3] In contrast to CO, the propene ligand both reduces electron density and increases steric hindrance at the metal. Thus inherently more reactive substrates (e.g., benzene, cyclopropane) or those that are not terribly hindered (e.g., *n*-butane) still undergo C–H insertion, but reaction with bulkier substrates such as cyclohexane now involves a higher energy barrier. The influence of steric hindrance on the rate of C–H activation also accounts for the slower rate at which the methyl-substituted allyl hydrides react with benzene.

In summary, the mechanisms outlined in Schemes XIX and XXIII are most consistent with our experimental observations. The major factor that distinguishes the system under study here from other C–H insertion reactions so far investigated is the ability of this system to transfer the hydrogen that has been abstracted from the activated hydrocarbon into a "receptor" ligand (the allyl group), preventing reversion of the C–H insertion reaction. Further investigation will be required to fully understand the nature of the differences in reactivity between the related C–H activating intermediates $(\eta^5$-$C_5Me_5)(PMe_3)Ir$ and $(\eta^5$-$Me_5)$(alkene)Ir.

Experimental Section

General. All manipulations were conducted under nitrogen or argon by standard drybox, Schlenk, or vacuum line techniques, unless otherwise noted. Experiments conducted in the drybox utilized a prescrubbed recirculating atmosphere of nitrogen in a Vacuum Atmospheres HE-533 Dri-Lab with attached MO-40-1 Dri-Train and equipped with a −40 °C freezer.

Infrared (IR) spectra were recorded on either a Perkin-Elmer Model 283 grating spectrometer or a Perkin-Elmer Model 1550 Fourier transform spectrometer equipped with a Model 7500 Professional Computer.

^{1}H NMR spectra were obtained at ambient temperature unless otherwise noted on either a Bruker AM-500 or a 300-MHz instrument assembled by Rudi Nunlist at the University of California, Berkeley, NMR facility. Chemical shifts are reported in units of parts per million (ppm) (δ) downfield from tetramethylsilane (Me_4Si). ^{1}H NMR shifts are recorded relative to residual protiated solvent: benzene-d_5, 7.15; cyclohexane-d_{11}, 1.38; tetrahydrofuran-d_7, 3.53 and 1.78; $CHDCl_2$, 5.32. ^{13}C NMR spectra were recorded at 75.5 or 125.7 MHz, and chemical shifts are given relative to the solvent resonance: benzene-d_6, 128.0; THF-d_8, 67.5. $^{31}P\{^1H\}$ NMR spectra were recorded at 121.5 MHz, and chemical shifts are given relative to external 85% H_3PO_4. All coupling constants are reported in hertz and multiplicities assigned as follows: s, singlet; d, doublet; t, triplet; q, quartet; m, multiplet.

Ultraviolet–visible spectra were recorded on a Hewlett-Packard Model 8450 UV/VIS spectrophotometer. Samples were prepared in the drybox and spectra recorded with use of a cuvette fused to a Kontes vacuum stopcock.

Mass spectra were obtained at the UCB mass spectrometry facility on AEI MS-12 and Finnigan 4000 mass spectrometers. Elemental analyses were performed by the UCB microanalytical laboratory. Melting points were recorded in sealed capillary tubes under nitrogen on a Thomas-Hoover capillary melting point apparatus and are uncorrected. Kinetic experiments were run in flame-sealed NMR tubes and were heated in either a Neslab Model RTE-8DD circulating water bath or a neslab Model EX-250 HT high-temperature oil bath.

Sealed NMR tubes were prepared by fusing Wilmad 505-PS 7 in. NMR tubes to glass joints which were subsequently attached to Kontes vacuum stopcocks. All samples were degassed by 3 freeze–pump–thaw cycles on a vacuum line. "Glass bombs" refer to cylindrical, medium walled Pyrex vessels joined to Kontes K-826510 high-vacuum Teflon stopcocks. Gas-phase mass measurements were performed by measuring the pressure in calibrated known-volume bulbs with a MKS Baratron connected to a high-vacuum line.

Unless otherwise stated, all solvents and reagents were purchased from commercial suppliers and used without further purification. Pentane and hexane were distilled from $LiAlH_4$, and CH_3CN from CaH_2 under nitrogen. Benzene, toluene, diethyl ether, and tetrahydrofuran were distilled from sodium benzophenone ketyl under nitrogen. Cumene (isopropylbenzene) and *n*-propylbenzene were washed with H_2SO_4, water, aqueous $NaHCO_3$, water, then brine. They were then dried first with $MgSO_4$ and then with sodium followed by distillation from sodium benzophenone ketyl prior to use. *n*-Butane and isobutane were dried over sodium and vacuum transferred. Benzene-d_6 and THF-d_8 were dried over benzophenone ketyl, cyclohexane-d_{12} was dried over sodium, acetone-d_6

(17) For examples of related bimetallic systems, see: (a) Bennett, M. A.; Donaldson, P. B. *Inorg. Chem.* **1978**, *17*, 1995. (b) Lee, W. S.; Brintzinger, H. H. *J. Organomet. Chem.* **1977**, *127*, 93. (c) Rosenblum, M.; North, B.; Wells, D.; Giering, W. P. *J. Am. Chem. Soc.* **1972**, *94*, 1239. (d) Caddy, P.; Green, M.; Smart, L. E.; White, N. *J. Chem. Soc., Chem. Commun.* **1978**, 839. (e) Dickson, R. D.; Johnson, S. H. *Aust. J. Chem.* **1976**, *29*, 2189. (f) Bennett, M. A.; Johnson, R. N.; Turney, T. W. *Inorg. Chem.* **1976**, *15*, 107. (g) Dickson, R. S.; Michel, L. J. *Au. J. Chem.* **1975**, *28*, 1943. (h) Dickson, R. S.; Kirsch, H. P. *Ibid.* **1974**, *27*, 61. (i) Andrews, P. S.; Gardner, S. A.; Rausch, M. D. *Inorg. Chem.* **1973**, *12*, 2396. (j) Rausch, M. D.; Andrews, P. S.; Gardner, S. A.; Siegel, A. *Organomet. Chem. Synth.* **1971**, *1*, 289. (k) McVey, S.; Maitlis, P. M. *J. Organomet. Chem.* **1969**, *19*, 169.

(18) (a) Nagashima, H.; Ara, K.-I.; Yamaguchi, K.; Itoh, K. *J. Organomet. Chem.* **1987**, *319*, C11. (b) Nagashima, H.; Yamaguchi, K.; Mukai, K.; Itoh, K. *Ibid.* **1985**, *291*, C20. (c) Nagashima, H.; Ohshima, T.; Itoh, K. *Chem. Lett.* **1984**, 789, 793.

(19) Stoutland, P. O.; Bergman, R. G. *J. Am. Chem. Soc.* **1985**, *107*, 4581.

was dried over Linde 4A molecular sieves, and CD_2Cl_2 was dried over CaH_2; all deuteriated solvents were vacuum transferred prior to use. 1,3,5-$C_6D_3H_3$ was purchased from MSD Isotopes and used as received. Trimethylphosphine (PMe_3) was purchased from Strem, dried over 1:5 Na:K alloy, and utilized exclusively by vacuum transfer. Triphenylphosphine (PPh_3) was purchased from Strem and recrystallized from hexane.

Synthesis of (η^5-C_5Me_5)Ir(η^3-C_3H_5)Cl (1). To a slurry of [(η^5-Me_5)$IrCl_2$]$_2$[5] (3.98 g, 5 mmol) in diethyl ether (150 mL, in a 250 mL round-bottomed flask) was added dropwise a 2 M solution of (allyl)MgCl (6.3 mL, 12.6 mmol) over a 10-min period, at ca. 19 °C, in the drybox. The reaction mixture was allowed to stir for 2 h, during which time the orange suspension slowly turned yellow. The flask was stoppered with a rubber septum and removed from the drybox. The reaction mixture was quenched with 100 μL of saturated NH_4Cl(aq) followed by filtration through a short pad of Celite. The Celite was washed with ca. 100 mL of toluene. The resulting yellow filtrate was concentrated in vacuo and the residue was crystallized from 1:1 toluene/hexane at −40 °C giving 2.76 g (6.8 mmol, 69%) of **1** as yellow, air stable, analytically pure needles: mp 164–165 °C; IR (KBr) 3060 (m), 3000 (s), 2980 (s), 2900 (s), 1500 (s), 1450 (s), 1385 (sh s), 1180 (m), 1075 (m), 1040 (s), 1039 (s), 1010 (m), 940 (sh s), 915 (sh m), 820 (m), 805 (m), 610 (m) cm^{-1}; ^1H NMR (C_6D_6) δ 3.89 (m, 1 H), 3.25 (d, J = 6.2 Hz, 2 H), 2.99 (d, J = 10 Hz, 2 H), 1.41 (s, 15 H); ^{13}C NMR (C_6D_6) δ 91.75 (s), 80.31 (d, J = 161.7 Hz), 45.24 (t, J = 160 Hz), 8.84 (q, J = 128.1 Hz); mass spectrometry, m/e 404, 363 (M^+, $M^+ - C_3H_5$). Anal. Calcd for $C_{13}H_{20}IrCl$: C, 38.65; H, 4.95; Cl, 8.78. Found: C, 38.91; H, 5.02; Cl, 8.49.

Synthesis of (η^5-C_5Me_5)Ir(η^3-C_3H_5)H (2). In the drybox a 250-mL round-bottomed flask was charged with 2.36 g (5.84 mmol) of the π-allyl chloride **1** and ca. 100 mL of diethyl ether. At box temperature (ca. 19 °C) 7.6 mL of $LiBEt_3H$ (1 M, 7.6 mmol) was added dropwise to the yellow slurry of **1**. The reaction was allowed to stir for 2 h during which time the slurry turned light brown and a white precipitate formed (LiCl). The reaction mixture was concentrated in vacuo giving a brown semisolid which after extraction into pentane gave a light-brown solution. This extract was filtered rapidly through a short pad of alumina packed into a medium pore frit and the alumina was washed with 100 mL of diethyl ether. The filtrate was concentrated, giving a light brown solid which after two crystallizations from pentane at −40 °C gave 1.37 g (3.71 mmol, 62% yield) of analytically pure, (π-allyl)iridium hydride **2**: mp (N_2) 68–70 °C dec; IR (KBr) 3040 (m), 2980 (s), 2900 (s), 2100 (s, Ir–H), 1470 (s), 1450 (s), 1380 (s), 1200 (m), 1070 (m), 1030 (s), 1000 (s), 945 (m), 925 (m), 825 (m), 810 (s), 640 (s), 400 (m), 365 (m); ^1H NMR (C_6D_6) δ 2.94 (m, 1 H), 2.53 (d, J = 5.7 Hz, 2 H), 2.24 (dd, J = 3.5, 8.7 Hz, 2 H), 1.86 (s, 15 H), −16.7 (br s, 1 H); ^1H NMR (C_6D_{12}) δ 2.77 (m, 1 H), 2.25 (d, J = 5.8 Hz, 2 H), 2.015 (s, 15 H), 1.765 (dd, J = 3.3, 8.6 Hz, 2 H), −17.28 (s, 1 H); ^{13}C NMR (C_6D_6) δ 91.3 (s), 64.9 (d, J = 162 Hz), 20.6 (t, J = 150 Hz), 10.4 (q, J = 127 Hz); mass spectrum, m/e 370, 368, 133 (M^+, $M^+ - H_2$, base); UV–vis (hexane) I_{max} = 246 nm (ε 3.6 × 10^4). Anal. Calcd for $C_{13}H_{21}Ir$: C, 42.28; H, 5.69. Found: C, 42.17; H, 5.73.

Synthesis of (η^5-C_5Me_5)Ir(PMe_3)(C_6H_5)n-C_3H_7 (3). A solution of the (π-allyl)iridium hydride **2** (23 mg, 0.062 mmol) in C_6H_6 (10 mL) was added to a Pyrex bomb in the drybox. The bomb was removed to a vacuum line and the solution was degassed. To this, PMe_3 was added (0.312 mmol) via vacuum transfer; the solution was then heated to 70 °C in an oil bath for 2 h. The resulting light orange solution was concentrated and the residue taken into the drybox. The products were dissolved in C_6D_6 and a ^1H NMR spectrum was taken. By the ^1H NMR spectrum two products were formed in a relative ratio of 10:1. The C_6D_6 was removed in vacuo and the residue was dissolved in 0.5 mL of hexane. This solution was passed through a short pad of silica gel packed into a glass pipet with 10% diethyl ether/hexane to wash the column. The filtrate was concentrated and the resulting white solid was crystallized from hexane at −40 °C, giving 20 mg (0.038 mmol, 62% yield) of analytically pure **3**: mp (N_2) 154–158 °C dec; IR (KBr) 3052 (m), 3038 (m), 2971 (m), 2943 (s), 2913 (s), 2856 (s), 2807 (s), 1568 (sh, s), 1473 (m), 1454 (m), 1374 (m), 1282 (s), 1170 (m), 1059 (m), 1022 (s), 950 (vs), 850 (m), 736 (s), 703 (s), 677 (m); ^1H NMR (C_6D_6) δ 7.46 (d, J = 6.8 Hz, 2 H), 7.22–7.12 (m, 3 H), 1.68–1.2 (n-propyl CH_2's, 4 H), 1.51 (d, J_{HP} = 1.7 Hz, 15 H), 1.31 (t, J = 6.4 Hz, 3 H), 1.08 (d, J_{HP} = 9.6 Hz, 9 H); ^{13}C NMR (C_6D_6) δ 139.9 (dd, J_{CP} = 3 Hz, J_{CH} = 153.4 Hz), 137.2 (d, J_{CP} = 12.4 Hz), 127.2 (dd, $^3J_{CH}$ = 6 Hz, obscured by solvent), 121.4 (dt, $^3J_{CH}$ = 7.5 Hz, J_{CH} = 157.3 Hz), 93.1 (d, J_{CP} = 3.4 Hz), 30.11 (dt, J_{CP} = 5.4 Hz, J_{CH} = 125.9 Hz), 21.44 (q, J_{CH} = 125.6 Hz), 15.34 (dq, J_{CP} = 36 Hz, J_{CH} = 129 Hz), 9.18 (q, J_{CH} = 126.6 Hz), 5.20 (dt, J_{CP} = 8.7 Hz, J_{CH} = 128 Hz); $^{31}P\{^1H\}$ NMR (C_6D_6) δ −40.22; mass spectrum, m/e 524, 481, 403 (M^+, $M^+ - C_3H_7$, base). Anal. Calcd for $C_{22}H_{36}IrP$: C, 50.48; H, 6.88. Found: C, 50.24; H: 7.04.

(η^5-C_5Me_5)Ir(PPh_3)(C_6H_5)n-C_3H_7 (4). A glass bomb was charged with 64 mg (0.173 mmol) of the (π-allyl)iridium hydride **2**, 63 mg (0.24 mmol) of PPh_3, and ca. 5 mL of C_6H_6. The resulting clear solution was removed to the vacuum line and degassed. The reaction mixture was heated to 45 °C for 24 h, during which time the solution turned light yellow. The volatile materials were removed in vacuo leaving a light yellow solid. The product was crystallized from toluene/hexane (1:1) at −40 °C giving 63 mg (0.089 mmol, 51%) of analytically pure **4** as light yellow microcrystals: mp (N_2) 160 °C slow dec; ^1H NMR (CD_2Cl_2) δ 7.4–7.2 (br, PPh_3), 6.75 (d, J = 7.1 Hz, 2 H), 6.71 (t, J = 7 Hz, 1 H), 6.60 (t, J = 7 Hz, 2 H), 1.48 (d, J_{HP} = 1.6 Hz, 15 H), 1.45–1.3, 1.15–1.05, 0.8–0.7 (m, n-propyl CH_2's, 4 H), 0.46 (t, J = 6.6 Hz, 3 H); $^{13}C\{^1H\}$ NMR (CD_2Cl_2) δ 139.6 (s), 132.6 (d, J_{CP} = 12 Hz), 126.5 (s), 120.7 (s), 134, 129.5, 127.5 (br, PPh_3), 30.1 (d, J_{CP} = 3.3 Hz), 20.6 (s), 11.4 (d, J_{CP} = 8.7 Hz), 9.25 (s); $^{31}P\{^1H\}$ NMR (CD_2Cl_2) δ 15.21; mass spectrum, m/e 710.667, 461 (M^+, $M^+ - C_3H_7$, base). Anal. Calcd for $C_{37}H_{42}IrP$: C, 62.63; H, 5.64. Found: C, 62.80; H, 5.80.

(η^5-C_5Me_5)Ir(PMe_3)(c-C_3H_5)n-C_3H_7 (5). In the drybox 49 mg (0.133 mmol) of **2** was weighed into a glass bomb. This was transferred to a vacuum line and ca. 3 mL of cyclopropane was added via vacuum transfer followed by the addition of PMe_3 (0.20 mmol). The glass bomb was wrapped with aluminum foil and then placed into an oil bath at 65 °C for 16.5 h. The resulting pale orange solution was concentrated in vacuo followed by crystallization of the residue from pentane at −40 °C. From this **5** was isolated as clear, analytically pure crystals in 39% yield (25 mg, 0.051 mmol): mp (N_2) slow dec above 130 °C; ^1H NMR (C_6D_6) δ 1.59 (d, J_{HP} = 1.7 Hz, 15 H), 1.4, 1.0, 0.8, 0.3, −0.1 (m, cyclopropyl and CH_2's of n-propyl), 1.15 (d, J_{HP} = 9.5 Hz, 9 H), 1.17 (obscured, methyl of n-propyl); ^{13}C NMR (C_6D_6) δ 92.61 (s), 30.98 (dt, J_{CP} = 4.9 Hz, J_{CH} = 121 Hz), 21.68 (q, J_{CH} = 122 Hz), 14.75 (dq, J_{CP} = 35.8 Hz, J_{CH} = 128 Hz), 8.80 (q, J_{CH} = 126 Hz), 4.72 (t, J_{CH} = 156 Hz), 3.00 (t, J_{CH} = 155 Hz), 2.06 (dt, J_{CP} = 9 Hz, J_{CH} = 124 Hz), −29.4 (dd, J_{CP} = 13.5 Hz, J_{CH} = 148 Hz); $^{31}P\{^1H\}$ NMR (C_6D_6) δ −39.76; mass spectrum, m/e 488, 445 (M^+, $M^+ - C_3H_7$ and base). Anal. Calcd for $C_{19}H_{36}IrP$: C, 46.80; H, 7.39 Found: C, 46.77; H, 7.55.

(η^5-C_5Me_5)Ir(PMe_3)(C_6H_5)Br (7). In the drybox 205 mg (0.364 mmol) of (η^5-C_5Me_5)Ir(PMe_3)Br_2[8] was dissolved in a minimal amount of benzene (ca. 20 mL) in a 100-mL RB flask. To this orange solution was added 20 mL of diethyl ether followed by the dropwise addition of phenylmagnesium chloride (0.2 mL, 0.4 mmol, 2 M) via syringe. The reaction was monitored by TLC (25% diethyl ether/hexane on silica gel) and after 14 h at box temperature (ca. 19 °C) the reaction was complete. The crude reaction was quenched by rapid filtration of the solution through a pad of silica gel packed into a medium pore frit with diethyl ether as an eluent. The resulting yellow solution was concentrated and chromatographed on silica gel with 25% diethyl ether/hexane. The front yellow band was collected, concentrated in vacuo, and then crystallized from toluene/hexane (1:1). The resulting air stable, orange crystals were analytically pure and isolated in 50% yield (102 mg, 0.182 mmol): mp 170–172 °C; IR (KBr) 3047 (m), 2979 (m), 2910 (s), 1569 (s), 1471 (m), 1455 (s), 1282 (s), 1021 (s), 956 (vs), 737 (s), 703 (s); ^1H NMR (CD_2Cl_2, 21 °C) δ 7.5 (br, 2 H), 6.9–6.8 (m, 3 H), 1.63 (d, J_{HP} = 2 Hz, 15 H, 1.47 (d, J_{HP} = 10.4 Hz, 9 H); ^1H NMR (CD_2Cl_2, −75 °C) δ 7.65 (d, J = 7.3 Hz, 1 H), 7.15 (d, J = 6.7 Hz, 1 H), 6.89–6.74 (m, 3 H), 1.63 (d, J_{HP} = 2 Hz, 15 H), 1.47 (d, J_{HP} = 10.4 Hz, 9 H); ^1H NMR (C_6D_6) δ 8.5–7.4 (br, 2 H), 7.2–7.0 (m, 3 H), 1.41 (d, J_{HP} = 2 Hz, 15 H), 1.18 (d, J_{HP} = 10.4 Hz, 9 H); $^{13}C\{^1H\}$ NMR (CD_2Cl_2, 21 °C) δ 141.2 (br s), 141 (obscured), 127.6 (s), 121.85 (s), 93.2 (d, J_{CP} = 4.5 Hz), 15.3 (d, J_{CP} = 38.9 Hz), 9.09 (s); $^{13}C\{^1H\}$ NMR (CD_2Cl_2, −75 °C) δ 141.6 (s), 140.6 (d, J_{CP} = 14.3 Hz), 139.1 (d, J_{CP} = 7.5 Hz), 127.1 (s), 126.4 (s), 120.9 (s), 92.1 (d, J_{CP} = 2.8 Hz), 14.25 (d, J_{CP} = 39.2 Hz), 8.50 (s); $^{31}P\{^1H\}$ NMR (CD_2Cl_2) δ −35.24; mass spectrum, m/e 560, 153 (M^+, base); UV–vis (CH_2Cl_2) λ_{max} = 326 (ε 1.5 × 10^3). Anal. Calcd for $C_{19}H_{29}IrBrP$: C, 40.73; H, 5.18. Found: C, 40.85; H, 5.26.

Synthesis of 3 from the Phenyliridium Bromide 7. In the drybox 32 mg (0.057 mmol) of **7** was dissolved in 20 mL of diethyl ether in a 50-mL RB flask. To this yellow solution was added n-propylmagnesium chloride (2 M, 0.1 mmol) dropwise via syringe. The reaction was allowed to stir for 24 h during which time the solution gradually cleared. The solution was concentrated, extracted into diethyl ether, filtered, and concentrated again leaving a clear oily residue. Analysis by ^1H NMR (C_6D_6) showed the production of **7** and (η^5-C_5Me_5)Ir(PMe_3)(C_6H_5)H in equivalent amounts. Chromatography on silica gel with 5% diethyl ether/hexane and collection of the first 25 mL of eluent followed by concentration in vacuo gave **3** >95% pure by ^1H NMR (9 mg, 0.017 mmol, 30% yield). The ^1H and $^{13}C\{^1H\}$ NMR spectra of **3** produced were identical with those obtained from **2**, PMe_3, and C_6H_6.

Thermolysis of (π-Allyl)iridium Hydride 2 in n-Butane. In the drybox 48 mg (0.130 mmol) of **2** was weighed into a pyrex bomb. The bomb was removed to a vacuum line and ca. 4 mL of n-butane was added via

vacuum transfer to the bomb containing **2**. The bomb was wrapped with aluminum foil and then the reaction mixture was heated to 60 °C for 2.5 days, during which time the solution turned brown. The volatile materials were removed in vacuo leaving a brown oil. The oil was dissolved in C_6D_6 and a ^1H NMR spectrum of the crude residue was recorded. Integration of the Ir–H resonances showed the production of two major iridium hydride products in a ratio of 9:1. The C_6D_6 solution was then concentrated in a sublimation apparatus. The reaction products were isolated by sublimation at ca. 40 °C and 10^{-4} Torr, and upon thawing, the white solid on the cold finger of the sublimation apparatus slowly melted. The ratio of **8a** to **8b** in the sublimed material remained 9:1 and was isolated in 40% yield (20 mg, 0.052 mmol) as a highly air sensitive light brown oil which solidified in the drybox freezer. The ^1H NMR (C_6D_6) and $^{13}C\{^1H\}$ NMR of the mixture of **8a** and **8b** were identical with those recorded in the independent synthesis (vida infra).

Thermolysis of 2 in Isobutane. In the drybox 20 mg (0.054 mmol) of **2** was weighed into a Pyrex bomb. The bomb was removed to the vacuum line and isobutane was added (ca. 4 mL) via vacuum transfer. The bomb was wrapped with aluminum foil and then heated to 70 °C for 7 days in an oil bath. The resulting brown solution was concentrated leaving a dark brown oil. The residue was extracted in pentane, filtered, and concentrated into a sublimation apparatus in the drybox. The 2-methylallyliridium hydride **9** (2.5 mg, 0.0065 mmol, 12% yield) was collected as a white solid by sublimation at 40 °C and 10^{-4} Torr and was identical with that obtained independently (vida infra) as determined by ^1H NMR spectroscopy and IR spectroscopy (benzene).

Synthesis of 8a and 8b from $(\eta^5\text{-}C_5Me_5)Ir(\eta^3\text{-}1\text{-}MeC_3H_4)Cl$. In the drybox 230 mg (0.551 mmol) of the 1-methallyliridium chloride[9] was weighed into a 100-mL round-bottomed flask. To this was added 50 mL of diethyl ether followed by the dropwise addition of 0.6 mL (0.6 mmol) of 1 M $LiBEt_3H$. The reaction was allowed to stir for 14 h during which time the yellow solution turned light brown with the deposition of a white solid. The crude reaction was concentrated, extracted into pentane, and filtered through a short plug of alumina packed in a medium pore frit. The filtrate was then concentrated leaving a light brown oil. A ^1H NMR spectrum (C_6D_6) was taken and the ratio of the two products was measured by integration as 3.2:1 and was >98% pure (134 mg, 0.350 mmol, 63.5% yield): IR (neat) 3040 (m), 2960 (s), 2900 (s), 2105 (s, Ir–H), 1475 (s), 1450 (s), 1385 (s), 1160 (s), 1115 (m), 930 (s), 770 (m), 710 (s); ^1H NMR (C_6D_6) of **8a** δ 2.80 (s, 1 H), 2.75 (m, 1 H), 2.37 (d, J = 5.3 Hz, 1 H), 2.21 (dd, J = 3, 7 Hz, 1 H), 1.85 (s, 15 H), 1.34 (d, J = 6.3 Hz, 3 H), −17.26 (br s, 1 H); for **8b** δ 3.42 (quintet, J = 6.4 Hz, 1 H), 3.15 (dt, J = 9.5, 6.5 Hz, 1 H), 2.66 (d, J = 6.3 Hz, 1 H), 2.61 (dd, J = 3.5, 9.4 Hz, 1 H), 1.85 (s, 15 H), 1.68 (dd, J = 6.6 Hz, 3 H), −17.02 (br s, 1 H); $^{13}C\{^1H\}$ NMR (assignments from ^{13}C (DEPT) NMR, C_6D_6) **8a** δ 91.15 (s, C_5Me_5), 68.61 (s, β-allylic CH), 30.76 (s, α-allylic CH), 19.76 (s, α-allylic CH_2), 19.65 (s, CH_3), 10.45 (s, C_5Me_5); **8b** δ 91.45 (s, C_5Me_5), 65.88 (s, β-allylic CH), 38.45 (s, α-allylic CH), 21.95 (s, CH_3), 19.35 (s, α-allylic CH_2), 10.33 (s, C_5Me_5); mass spectrum, m/e 384, 382 (M^+, $M^+ - H_2$ and base). Anal. Calcd for $C_{14}H_{23}Ir$: C, 43.84; H, 6.00. Found: C, 44.06; H, 6.14.

Synthesis of $(\eta^5\text{-}C_5Me_5)Ir(\eta^3\text{-}2\text{-}MeC_3H_4)Cl$ (10). A 100-mL round-bottomed flask was charged with 360 mg (0.496 mmol) of $[(\eta^5\text{-}C_5Me_5)IrCl_2]_2$ and to this was added 50 mL of diethyl ether under a nitrogen atmosphere. To this orange slurry was added 1.25 mmol of 2-methallylmagnesium chloride (prepared from 2-methyl-3-chloropropene and magnesium in diethyl ether at −10 °C) dropwise via syringe. The reaction was allowed to stir for 2 h at room temperature during which time the slurry turned into a yellow solution and a white solid. The reaction was quenched by the addition of 100 μL of saturated NH_4Cl. The crude mixture was filtered through a short plug of Celite packed into a medium pore frit, the Celite was washed with toluene, and the filtrate was concentrated in vacuo leaving a yellow residue. The residue was crystallized from toluene/hexane (1:1) giving 240 mg (0.575 mmol, 58% yield) of bright yellow needles of **10**: mp 192–193 °C dec; IR (KBr) 3046 (m), 2991 (s), 2979 (s), 2957 (s), 2913 (s), 1504 (m), 1458 (s), 1445 (m), 1431 (m), 1382 (s), 1033 (m), 1020 (s), 850 (s), 827 (m), 591 (m); ^1H NMR ($CDCl_3$) δ 3.40 (s, 2 H), 2.59 (s, 2 H), 1.89 (s, 3 H), 1.86 (s, 15H); ^{13}C NMR ($CDCl_3$) δ 95.1 (s), 91.8 (s), 45.2 (t, J = 157 Hz), 24.0 (q, J = 127 Hz), 9.17 (q, J = 128.1 Hz); mass spectrum, m/e 418, 363 (M^+, $M^+ - C_4H_7$ base); UV–vis (CH_2Cl_2) λ_{max} = 298, 392 nm (ϵ 2.5 × 10^3, 250). Anal. Calcd for $C_{14}H_{22}IrCl$: C, 40.23; H, 5.27; Cl, 8.49. Found: C, 39.98; H, 5.32; Cl, 8.61.

Synthesis of $(\eta^5\text{-}C_5Me_5)Ir(\eta^3\text{-}2\text{-}MeC_3H_4)H$ (9). In the drybox 170 mg (0.407 mmol) of **10** was weighed into a 100-mL round-bottomed flask. To this was added 40 mL of diethyl ether followed by the dropwise addition of $LiBEt_3H$ (0.5 mL, 1 M, 0.5 mmol) via syringe. The reaction was allowed to stir at box temperature for 14 h during which time the yellow solution turned light brown with the deposition of a white solid. The reaction mixture was concentrated, extracted into pentane, and then filtered through a short plug of alumina packed into a medium frit. The alumina was washed with ca. 20 mL of diethyl ether. The filtrate was concentrated leaving a light brown solid which was crystallized from pentane at −40 °C giving 129 mg (0.337 mmol, 83%) of the iridium hydride **9** as analytically pure air sensitive, clear crystals: mp (N_2) 51.5–52.5 °C; IR (C_6D_6) 2117 (Ir–H); ^1H NMR (C_6D_6) δ 2.41 (s, 2 H), 2.31 (d, J = 3.1 Hz, 2 H), 1.89 (s, 3 H), 1.84 (s, 15 H), −17.3 (br s, Ir–H); $^{13}C\{^1H\}$ NMR δ 91.6 (s), 74.5 (s), 22.75 (s), 20.5 (s), 10.6 (s); mass spectrum (15 eV), m/e 384 (M^+ and base). Anal. Calcd for $C_{14}H_{23}Ir$: C, 43.84; H, 6.00. Found: C, 43.76; H, 6.14.

Thermolysis of 8a and 8b in Benzene with Added PMe_3: Synthesis of $(\eta^5\text{-}C_5Me_5)Ir(PMe_3)(C_6H_5)n\text{-}C_4H_9$ (11). In the drybox 23 mg (0.060 mmol) of a 3:1 mixture of **8a**:**8b** was weighed into a Pyrex bomb followed by the addition of 2 mL of C_6H_6. The bomb was removed to a vacuum line and the solution was degassed. To this solution was added 0.10 mmol of PMe_3 via vacuum transfer. The bomb was wrapped with aluminum foil and the reaction mixture was heated to 80 °C for 20 h. The volatile materials were removed leaving a light orange, oily residue which slowly solidified. This residue was crystallized from pentane at −40 °C giving 15 mg of **11** (47% yield, 0.028 mmol) as air stable clear crystals: mp (N_2) 74–78 °C; ^1H NMR (C_6D_6), δ 7.44 (dd, J = 1.3, 8.0 Hz, 2 H), 7.2–7.09 (m, 3 H), 1.69–1.56 and 1.53–1.38 (m, CH_2's of n-butyl group), 1.50 (d, J_{HP} = 1.7 Hz, 15 H), 1.13 (t, J = 7.2 Hz, 3 H), 1.08 (d, J_{HP} = 9.5 Hz, 9 H); $^{13}C\{^1H\}$ NMR (C_6D_6) δ 139.9 (d, J_{CP} = 2.7 Hz), 137.2 (d, J_{CP} = 12 Hz), 127.2 (s), 121.4 (s), 93.1 (d, J_{CP} = 2.3 Hz), 39.7 (d, J_{CP} = 4.3 Hz), 29.8 (s), 15.3 (d, J_{CP} = 36 Hz), 14.5 (s), 9.18 (s), 1.63 (d, J_{CP} = 8.8 Hz); $^{31}P\{^1H\}$ NMR (C_6D_6) δ −40.3; mass spectrum, m/e 538, 481, 44 (M^+, $M^+ - C_4H_7$, base). Anal. Calcd for $C_{23}H_{38}IrP$: C, 51.38; H, 7.07. Found: C, 51.62; H, 7.22.

Thermolysis of 9 in C_6H_6 with Added PMe_3: Synthesis of $(\eta^5\text{-}C_5Me_5)Ir(PMe_3)(C_6H_5)i\text{-}C_4H_9$ (12). In the drybox 35 mg (0.091 mmol) of **9** and 2 mL of C_6H_6 were added to a Pyrex bomb. The bomb was removed to the vacuum line and the solution was degassed followed by the addition of PMe_3 (0.15 mmol) via vacuum transfer. The bomb was wrapped with aluminum foil and the reaction mixture was heated to 100 °C for 4 h. The volatile materials were removed in vacuo and the orange residue was taken up in C_6D_6. A ^1H NMR spectrum was recorded and showed the production of **12**, $(\eta^5\text{-}C_5Me_5)Ir(PMe_3)(C_6H_5)H$, and the bisphosphine complex **6** in a ratio of 3.5:2.1. In the drybox the C_6D_6 solution of the reaction mixture was filtered through a short pad of silica gel packed in a glass pipet with diethyl ether to wash the silica gel. The filtrate was collected and concentrated and the residue crystallized twice from pentane at −40 °C in the drybox freezer giving analytically pure, clear crystals of **12** (13 mg, 0.024 mmol, 27% yield): mp (N_2) ~129 °C dec without melting; IR (KBr) 3053 (m), 2944 (s), 2911 (s), 2854 (s), 2795 (w), 1569 (m), 1473 (m), 1455 (m), 1281 (m), 952 (s), 736 (s), 705 (s); ^1H NMR (C_6D_6) δ 1.8 and 1.6 (m, 3 H), 1.48 (d, J_{HP} = 1.8 Hz, 15 H), 1.22 (d, J = 6.1 Hz, 3 H), 1.15 (d, J = 6.1 Hz, 3 H), 1.11 (d, J_{HP} = 9.4 Hz, 9 H); $^{13}C\{^1H\}$ NMR δ 140.2 (d, J_{CP} = 3 Hz), 138 (d, J_{CP} = 12.5 Hz), 127.2 (s), 121.4 (s), 93.5 (br s), 33.6 (d, J_{CP} = 4.6 Hz), 28.0 (s), 27.1 (s), 15.9 (d, J_{CP} = 35.5 Hz), 12.2 (d, J_{CP} = 9.2 Hz), 9.7 (s); $^{31}P\{^1H\}$ NMR (C_6D_6) δ −41.27; mass spectrum, m/e 538, 481, 403 (M^+, $M^+ - C_4H_9$, base). Anal. Calcd for $C_{23}H_{38}IrP$: C, 51.38; H, 7.07. Found: C, 51.62; H, 7.10.

Synthesis of $(\eta^5\text{-}C_5Me_5)Ir(PMe_3)_2$ (6). In the drybox 100 mg (0.27 mmol) of the (π-allyl)iridium hydride **2** and 15 mL of hexane were added to a Pyrex bomb. The bomb was removed to a vacuum line and 10.83 mmol of PMe_3 was added via vacuum transfer. The clear solution was irradiated for 5.25 h at ca. 6 °C during which time the solution turned bright orange. The volatile materials were removed in vacuo leaving a bright orange residue which was crystallized from hexane at −40 °C giving 95 mg (0.20 mmol, 74% yield) of **6** as highly air sensitive orange crystals: mp (N_2) 102–103 °C; ^1H NMR (C_6D_6) δ 2.07 (t, J_{HP} = 1.0 Hz, 15 H), 1.43 (d, $^2J_{HP} + {}^4J_{HP}$ = 8.7 Hz, 9 H); $^{13}C\{^1H\}$ NMR (C_6D_6) δ 91.62 (br s), 25.5 (five line pattern), 12.39 (s); $^{31}P\{^1H\}$ NMR (C_6D_6) δ −54.35; mass spectrum, m/e 480 (M^+ and base); UV–vis (hexane) λ_{max} = 272, 315, 352 nm (ϵ 7.5 × 10^3, 4.9 × 10^3, 3.3 × 10^3). Anal. Calcd for $C_{16}H_{33}IrP_2$: C, 40.09; H, 6.88. Found: C, 39.87; H, 6.90.

Protonation of 6 with HBF_4. In the drybox 26 mg (0.054 mmol) of the bisphosphine complex **6** was weighed into a 25-mL round-bottom flask. To this was added 10 mL of diethyl ether followed by the dropwise addition of an excess of $HBF_4 \cdot Et_2O$ resulting in the immediate deposition of a white solid. The solid was collected via filtration and was washed with diethyl ether giving 25 mg (0.044 mmol, 82% yield) of $(\eta^5\text{-}C_5Me_5)Ir(PMe_3)_2H^+BF_4^-$ and was judged to be pure by ^1H NMR spectroscopy: ^1H NMR (acetone-d_6) δ 2.09 (t, J_{HP} = 1.7 Hz), 1.79 (vt, $^2J_{HP} + {}^4J_{HP}$ = 10.4 Hz), −17.8 (t, J_{HP} = 30.6 Hz); $^{13}C\{^1H\}$ NMR (acetone-d_6) δ 98.43 (s), 21.4 (five-line pattern), 10.73 (s). Literature values:[14] ^1H NMR (acetone-d_6) δ 2.09 (t, J_{HP} = 2.0 Hz, 15 H), 1.80 (vt, $^2J_{HP} + {}^4J_{HP}$ = 10.1 Hz, 9 H), −17.78 (t, J_{HP} = 30.1 Hz, 1 H); $^{13}C\{^1H\}$

NMR (acetone-d_6) δ 98.4 (s), 21.4 (five-line pattern), 10.7 (s).

Irradiation of 8a and 8b in the Presence of PMe_3. In the drybox 20 mg (0.052 mmol) of a 9:1 mixture of **8a** and **8b**, 4 mg of ferrocene, and 0.60 mL of C_6D_6 were added to a NMR tube fused to a glass joint. The tube was fitted with a Kontes vacuum stopcock and was removed to a vacuum line. The solution was degassed followed by the addition of PMe_3 (0.35 mmol). The tube was flame sealed under vacuum. The reaction mixture was irradiated for 6.5 h (reaction monitored by ^1H NMR); by ^1H NMR and $^{31}P\{^1H\}$ NMR analysis **6** was the only organometallic product observed (93% yield as determined by integration of η^5-C_5Me_5 resonance versus ferrocene). A mixture of *trans*- and *cis*-butene (12:1 relative ratio) was formed in 67% yield (versus ferrocene) along with minor amounts of unidentified volatile materials.

Thermolysis of 2 in *n*-Propylbenzene: Synthesis of (η^5-C_5Me_5)Ir(η^3-1-PhC_3H_4)H (14) and (η^5-C_5Me_5)Ir(η^1-η^2-CH_2=$CHCH_2$-C_6H_4)H (13). In the drybox 64 mg of **2** (0.17 mmol) was weighed into a Pyrex bomb. The bomb was removed to a vacuum line and ca. 10 mL of *n*-propylbenzene was vacuum transferred onto **2**. The bomb was wrapped with aluminum foil and the reaction mixture was heated to 65 °C for 45 h during which time the solution turned light brown. The volatile materials were removed in vacuo leaving a brown oil. The oil was taken into the drybox and dissolved in C_6D_6 and a ^1H NMR spectrum recorded. The spectrum showed the presence of two products in a ratio of 4:1 (determined by integration of Ir–H resonances). The major product was obtained by two crystallizations from pentane at −40 °C in the drybox freezer giving 34 mg (0.076 mmol, 44% yield) of clear, air-sensitive crystals of **13**. The minor product was assigned as **14** based on its ^1H and $^{13}C\{^1H\}$ NMR spectra taken as a mixture with **13**. For **13**: mp (N_2) 94–95 °C; IR (KBr) 3041 (s), 2994 (s), 2984 (s), 2893 (s), 2826 (m), 2126 (sh s, Ir–H), 1577 (sh s), 1558 (m), 1451 (s), 1432 (m), 1383 (s), 1030 (s), 764 (s), 737 (s), 682 (s); ^1H NMR (C_6D_6) δ 7.43 (m, 1 H), 7.12 (m, 1 H), 7.0–6.95 (m, 2 H), 3.35 (dd, J = 6.2, 16.7 Hz, 1 H), 3.04 (d, J = 16.7 Hz, 1 H), 2.84 (m, 2 H), 2.52 (d, J = 7.3 Hz, 1 H), 1.62 (s, 15 H), −15.27 (s, 1 H); ^1H NMR (C_6D_{12}) δ 6.97 (dd, J = 1.2, 7.2 Hz, 1 H), 6.70 (d, J = 7.2 Hz, 1 H), 6.53 (m, 1 H), 6.47 (m, 1 H), 3.18 (dd, J = 6.7, 16.5 Hz, 1 H), 2.92 (m, 1 H), 2.82 (d, J = 16.6 Hz, 1 H), 2.52 (d, J = 10.2 Hz, 1 H), 2.44 (d, J = 8.1 Hz, 1 H), 1.90 (s, 15 H), −15.53 (s, 1 H); ^{13}C NMR (C_6D_6) δ 155.3 (s), 139.2 (br s), 139.9 (d, J = 153,5 Hz), 124.7 (dd, ^3J = 7.5 Hz, J = 154.4 Hz), 123.5 (dd, ^3J = 6.2 Hz, J = 151 Hz), 122.8 (dd, ^3J = 7.7 Hz, J = 157.2 Hz), 95.0 (s), 54.0 (d, J = 153 Hz), 38.98 (t, J = 125.3 Hz), 27.8 (t, J = 157.7 Hz), 9.4 (q, J = 127 Hz); mass spectrum (15 eV), m/e 446 (M^+ and base). Anal. Calcd for $C_{19}H_{25}Ir$: C, 51.21; H, 5.62. Found: C, 51.35; H, 5.57. Resonances assigned to **14**: ^1H NMR (C_6D_6) δ 7.1–6.97 (m, 5 H), 4.06 (dd, J = 2.8, 8.5 Hz, 1 H), 3.75 (m, 1 H), 2.45 (d, J = 6 Hz, 1 H), 2.43 (dd, J = 3.7, 8.6 Hz, 1 H), 1.61 (s, 15 H), −16.72 (br s, 1 H); $^{13}C\{^1H\}$ NMR (C_6D_6) δ 144.8 (s), 128.6 (s), 127.9 (s), 123.9 (s), 91.7 (s), 62.2 (s), 38.2 (s), 19.7 (s), 9.9 (s).

(η^5-C_5Me_5)(L)IrCH(CH_3)CH_2-C_6H_4, L = PPh_3 (15). In the drybox 17 mg of PPh_3 (0.065 mmol) was added to a C_6H_6 (5 mL) solution of **13** (21 mg, 0.047 mmol). The reaction mixture was allowed to stir for 15 min followed by the removal of the volatile materials in vacuo. The residue was dissolved in C_6D_6 and a ^1H NMR spectrum was recorded showing two new η^5-C_5Me_5 resonances in a ratio of 22:1. The resulting pale yellow residue was recrystallized from toluene/hexane (1:1) at −40 °C giving 18 mg (0.025 mmol, 54% yield) of analytically pure **15**: mp (N_2) 174–178 °C dec; IR (KBr) 3048 (m), 2977 (m), 2903 (s), 2850 (s), 2810 (m), 1574 (m), 1481 (m), 1447 (m), 1434 (s), 1092 (m), 1028 (m), 1018 (m), 742 (s), 698 (s), 539 (s), 513 (s); ^1H NMR (C_6D_6) δ 7.34 (d, J = 7.3 Hz, 1 H), 7.28 (d, J = 7.3 Hz, 1 H), 7.05 (t, J = 7.2 Hz, 1 H), 6.83 (d, J = 7.4 Hz, 1 H), 7.3–7.1, 7.05–6.95 (br, PPh_3), 3.2–3.0 (m, 3 H), 1.64 (d, J = 6.6 Hz, 3 H), 1.47 (d, J_{HP} = 1.9 Hz, 15 H); ^1H NMR (THF-d_8) δ 7.4–6.9 (br, PPh_3), 6.90 (d, J = 7.3 Hz, 1 H), 6.85 (d, J = 7.1 Hz, 1 H), 6.59 (t, J = 7.3 Hz, 1 H), 6.36 (t, J = 7.4 Hz, 1 H), 2.75–2.6 (m, 3 H), 1.50 (d, J_{HP} = 1.9 Hz, 15 H), 1.37 (d, J = 6.2 Hz, 3 H); $^{13}C\{^1H\}$ NMR (THF-d_8) δ 157.2 (s), 143.7 (d, J_{CP} = 12.5 Hz), 138.3 (d, J_{CP} = 2.8 Hz), 135 (d, J_{CP} = 9.8 Hz), 130.0 (s), 128.1 (d, J_{CP} = 9.7 Hz), 124.3 (s), 121.9 (s), 121.7 (s), 95.4 (d, J_{CP} = 3.4 Hz), 53.6 (s), 25.9 (s), 10.9 (d, J_{CP} = 6 Hz), 9.7 (s); $^{31}P\{^1H\}$ NMR (C_6D_6) δ 14.4; $^{31}P\{^1H\}$ NMR (CD_2Cl_2) δ 13.6; mass spectrum, m/e 708, 590 (M^+, base). Anal. Calcd for $C_{37}H_{40}IrP$: C, 62.79; H, 5.66. Found: C, 63.03; H, 5.80. Minor Isomer: $^{31}P\{^1H\}$ NMR δ 9.68.

L = PMe_3 (16). In the drybox a solution of **13** (18 mg, 0.041 mmol) in pentane was added to a Pyrex bomb. The bomb was removed to a vacuum line and the solution was degassed followed by the addition of PMe_3 via vacuum transfer (0.065 mmol). The reaction mixture was allowed to stir at room temperature for 15 min. The volatile materials were removed in vacuo leaving a white solid. Crystallization from pentane at −40 °C gave 20 mg (0.038 mmol, 95% yield) of an 8:1 ratio of stereoisomers of **16** as analytically pure clear crystals (ratio identical with that observed in the crude reaction mixture). Major isomer: ^1H NMR (C_6D_6) δ 7.38 (d, J = 7.1 Hz, 1 H), 7.24 (d, J = 7.2 Hz, 1 H), 7.10 (t, J = 7.2 Hz, 1 H), 7.00 (t, J = 7.2 Hz), 3.25 (dd, J = 5.4, 14.4 Hz, 1 H), 3.05 (t, J = 13.7 Hz, 1 H), 2.40 (m, 1 H), 1.75 (d, J = 7.2 Hz, 3 H), 1.63 (d, J_{HP} = 1.9 Hz, 15 H), 0.865 (d, J_{HP} = 9.5 Hz, 9 H); $^{13}C\{^1H\}$ NMR (C_6D_6) δ 157.3 (s), 148.1 (d, J_{CP} = 13.7 Hz), 137.2 (d, J_{CP} = 3.8 Hz), 124.5 (s), 121.9 (s), 121.2 (s), 93.1 (d, J_{CP} = 3.6 Hz), 53.5 (s), 27.2 (s), 14.6 (d, J_{CP} = 37.6 Hz), 10.0 (s), 7.73 (d, J_{CP} = 7.6 Hz); $^{31}P\{^1H\}$ NMR (C_6D_6) δ −34.4. Minor isomer: ^1H NMR (C_6D_6, partial) δ 3.38 (dd, J = 7.7, 16.4 Hz, 1 H), 3.15 (m, 1 H), 2.83 (dd, J = 10, 16.4 Hz, 1 H), 1.58 (d, J_{HP} = 1.6 Hz, η^5-C_5Me_5), 0.98 (d, J_{HP} = 9.7 Hz, PMe_3); $^{31}P\{^1H\}$ NMR (C_6D_6) δ −37.4. Mixture of isomers: mass spectrum, m/e 522, 405 (M^+, base). Anal. Calcd for $C_{22}H_{34}IrP$: C, 50.65; H, 6.52. Found: C, 50.61; H, 6.68.

L = *t*-BuNC (17). With use of the same procedure as with L = PMe_3, a 54% isolated yield of one stereoisomer was obtained after crystallization from pentane at −40 °C in the drybox freezer. Major isomer: mp (N_2) 137–137.5 °C; IR (KBr) 3040 (m), 2980 (s), 2833 (m), 2100 (s), 2057 (s, CN), 1448 (m), 1209 (m), 737 (sh, s); ^1H NMR (C_6D_6) δ 7.52 (dd, J = 1.8, 6.7 Hz, 1 H), 7.41 (br d, J = 6.2 Hz, 1 H), 7.15–7.06 (m, 2 H), 3.41–3.3 (m, 2 H), 3.06 (t, J = 13.5 Hz, 1 H), 1.86 (d, J = 7 Hz, 3 H), 1.73 (s, 15 H), 0.93 (s, 9 H); ^{13}C NMR (C_6D_6) δ 157.2 (s), 143.2 (s), 142.9 (s), 137.9 (dd, ^3J = 6.7, J = 153 Hz), 124.6 (dd, ^3J = 7.5, J = 154 Hz), 122.9 (dd, ^3J = 7.7, J = 155 Hz), 121.9 (br d, J = 150 Hz), 95.2 (s), 56.1 (s), 53.4 (t, J = 122 Hz), 31.7 (q, J = 127.6 Hz), 26.9 (q, J = 123.5 Hz), 12.0 (d, J = 131 Hz), 9.74 (q, J = 127 Hz); mass spectrum, m/e 529, 57 (M^+, base). Anal. Calcd for $C_{24}H_{34}IrN$: C, 54.52; H, 6.44; N, 2.65. Found: C, 54.65; H, 6.56; N, 2.56. Approximately 19% of the minor diastereomer was observed in the crude product: ^1H NMR (C_6D_6, aromatic region obscured by major isomer) δ 3.53 (dd, J = 6, 15 Hz, 1 H), 3.15 (dd, J = 9.7, 14.9 Hz, 1 H), 2.72 (m, 1 H), 1.89 (d, J = 7 Hz, 3 H), 1.71 (s, 15 H), 0.90 (s, 9 H); $^{13}C\{^1H\}$ NMR (C_6D_6) δ 136.9 (s), 124.8 (s), 122.5 (s), 121.6 (s), 95.1 (s), 54.1 (s), 31.2 (s), 28.9 (s), 19.3 (s), 9.1 (s).

Addition of 2-Butyne to 13: Synthesis of 18. In the drybox 28 mg (0.063 mmol) of **13** and ca. 3 mL of hexane were added to a glass bomb. The bomb was sealed and removed to the vacuum line and the solution was degassed. To this was added 1.5 equiv (0.1 mmol) of 2-butyne via vacuum transfer. The solution was allowed to stir at room temperature for 24 h after which time the volatile materials were removed in vacuo leaving a white residue. The residue was taken into the drybox and dissolved in pentane, and upon cooling to −40 °C clear, analytically pure crystals of **18** formed (15 mg, 0.03 mmol 48%): mp (N_2) 121–124 °C; IR (KBr) 2970 (s), 2886 (s), 1489 (s), 1464 (s), 1445 (s), 1378 (s), 1029 (s), 763 (s), 743 (s); ^1H NMR (C_6D_6) δ 7.3–7.0 (m, aromatic, 4 H), 3.81 (dd, J = 2.1, 16 Hz, 1 H), 3.39 (dd, J = 3.6, 16 Hz, 1 H), 2.76 (m, 1 H), 2.62 (q, J = 6.7 Hz, 1 H), 1.69 (d, J = 6.7 Hz, 3 H), 1.64 (s, 3 H), 1.56 (dd, J = 1.7, 8.2 Hz, 1 H), 1.50 (s, 15 H), 0.64 (dd, J = 1.8, 10 Hz, 1 H); ^{13}C NMR (C_6D_6) δ 145.1 (s), 135.5 (s), 131 (dd, ^3J = 6.6, J = 154.6 Hz), 128.6 (br d, J = 152 Hz), 127.6 (dd, ^3J = 7.6 Hz, obscured by solvent), 125.3 (dd, ^3J = 7.8 Hz, J = 158 Hz), 94.6 (s), 42.6 (d, J = 149 Hz), 37.6 (s), 35.3 (t, J = 126 Hz), 32.4 (d, J = 151 Hz), 27.8 (t, J = 154.3 Hz), 27.6 (q, J = 125.2 Hz), 17.2 (q, J = 124.7 Hz), 9.0 (q, J = 126.7 Hz); mass spectrum, m/e 500 (M^+ base). Anal. Calcd for $C_{23}H_{31}Ir$: C, 55.29; H, 6.21. Found: C, 55.18; H, 6.26.

Thermolysis of 2 in Cumene: Synthesis of (η^5-C_5Me_5)Ir(η^3-2-PhC_3H_4)H (19) and the Diirdium Dimer 20. In the drybox 112 mg (0.303 mmol) of **2** was weighed into a Pyrex bomb. The bomb was removed to a vacuum line and ca. 20 mL of cumene was added via vacuum transfer. The bomb was wrapped with aluminum foil and the solution was heated to 65 °C for 48 h during which time the solution turned wine red. The volatile materials were removed in vacuo leaving a red residue. By ^1H NMR (C_6D_6) two new products were formed in a 1:1 ratio. Chromatography on alumina separated the two products. The first fraction was eluted with benzene as a pale yellow solution. This was concentrated and the residue crystallized from pentane at −40 °C, giving **19** ca. 95% pure by ^1H NMR spectroscopy (19 mg, 0.043 mmol, 14% yield). The second fraction eluted with diethyl ether as a red solution which was concentrated and then crystallized from pentane at −40 °C, giving **20** in 20% yield (23 mg, 0.030 mmol). Improvement in the isolated yield of **20** was accomplished by the thermolysis of **2** (57 mg, 0.154) in 5 mL of cumene for 3 days giving 26 mg (0.034 mmol, 44% yield) of pure material after crystallization from pentane. For **19**: IR (KBr) 2157 (s, Ir–H); ^1H NMR (C_6D_6) δ 7.30 (d, J = 7.3 Hz, 2 H), 7.14 (t, J = 7.6 Hz, 2 H), 6.96 (t, J = 6.9 Hz, 1 H), 3.27 (s, 2 H), 2.29 (d, J = 2.5 Hz, 2 H), 1.60 (s, 15 H), −17.0 (s, 1 H); $^{13}C\{^1H\}$ NMR δ 141.3 (s), 128.4 (s), 124.9 (s), 126.1 (s), 93.0 (s), 72.2 (s), 14.4 (s), 9.87 (s); MS m/e 446, 444, 429 (M^+, $M^+ - H_2$, base). For **20**: mp (N_2) 218–221 °C; IR (KBr) 2906 (s), 1453 (m), 1377 (s), 1289 (m), 1031 (s), 745 (s); ^1H NMR (C_6D_6) δ 7.46 (d, J = 8.1 Hz, 1 H), 7.01 (d, J = 8.7 Hz, 1 H),

Table V. Crystal and Data Collection Parameters[a,b] for **20** (Empirical Formula $Ir_2C_{29}H_{38}$)

(A) Crystal Parameters at T = 26 °C

a = 19.6009 (18) Å	space group: $P2_1/c$
b = 0.6466 (11) Å	formula weight = 771.0 amu
c = 15.3132 (16) Å	Z = 4
α = 90.0°	d_c = 1.99 g cm^{-3}
β = 92.639 (8)°	μ(calcd) = 102.8 cm^{-1}
γ = 90.0°	size: 0.095 × 0.16 × 0.35 mm
V = 2579.3 (9) Å^3	

(B) Data Measurement Parameters

radiation: Mo Kα (λ = 0.71073 Å)
monochromator: highly oriented graphite (2θ = 12.2)
detector: crystal scintillation counter, with PHA
reflections measured: $\pm k,+k,+l$
2θ range: 3 → 45°
scan type: $q - 2\theta$
scan width: $\Delta\theta$ = 0.70 (θ, deg/min)
scan speed: 0.85 → 6.70 (θ, deg/min)
background: measured over 0.25(scan width) added to each end of the scan
vert. aperture = 4.0 mm
horiz. aperture = 2.5 + 1.0 tan (θ) mm
no of reflections collected: 3766
no. of unique reflections: 3354
intensity standards: (−3,3,9), (12,2,2), (5,4,6); measured every 1 h of X-ray exposure time; over the data collection period 2% decrease in intensity was observed
orientation: three reflections were checked after every 150 measurements; crystal orientation was redetermined if any of the reflections were offset by more than 0.10° from their predicted positions; reorientation was performed two times during data collection

[a] Unit cell parameters and their esd's were derived by a least-squares fit to the setting angles of the unresolved Mo Kα components of 24 reflections with $2t$ near 28°. [b] In this and all subsequent tables the esd's of all parameters are given in parentheses, right-justified to the least significant digit(s) of the reported value.

6.88 (dd, J = 6.8, 8.9 Hz, 1 H), 6.71 (dd, J = 7.1, 8.3 Hz, 1 H), 6.49 (s, 1 H), 2.12 (s, 15 H), 2.09 (s, 3 H), 1.48 (s, 15 H); $^{13}C\{^1H\}$ NMR (C_6D_6, assigned by DEPT experiment) δ 145.5 (CH), 124.4 (CH), 123.0 (CH), 121.9 (C), 121.1 (CH), 120.5 (CH), 107.4 (C), 97.5 (C), 86.8 (C), 85.4 (C), 16.2 (CH_3), 11.2 (CH_3), 8.80 (CH_3); mass spectrum, m/e 770, 69 (M^+, base); UV-vis (hexane) λ_{max} 325 (ϵ 5 × 10^3), 381 (ϵ 3.8 × 10^3), 500 (ϵ 1.5 × 10^3). Anal. Calcd for $C_{29}H_{38}Ir_2$: C, 45.17; H, 4.93. Found: C, 45.37; H, 5.06.

X-ray Diffraction Study of Diiridium Complex 20. The structure analysis was performed by Dr. F. J. Hollander. Blocky, platelike, red crystals of **20** were obtained by slow evaporation of diethyl ether from a diethyl ether/acetonitrile solution in the drybox. Fragments cleaved from the tips of some of these crystals were mounted on glass fibers with polycyanoacrylate cement.

The crystal used for data collection was transferred to our Enraf-Nonius CAD-4 diffractometer[20] and centered in the beam. Automatic peak search and indexing procedures yielded a monoclinic reduced primitive cell. Inspection of the Niggli values[20] revealed no conventional cell of higher symmetry. The final cell parameters and specific data collection parameters for this data set are given in Table V.

The 3766 raw intensity data were converted to structure factor amplitudes and their esds by correction for scan speed, background, and Lorentz and polarization effects. Inspection of the intensity standards revealed a reduction of 2% of the original intensity. The data were corrected for this decay. Inspection of the azimuthal scan data showed a variation I_{min}/I_{max} = 0.65 for the average curve. An absorption correction based on the measured shape and size of the crystal and on the 10 × 24 × 6 Gaussian grid of internal points was applied to the data (T_{max} = 0.376, T_{min} = 0.214). Inspection of the systematic absences indicated uniquely space group $P2_1/c$. Removal of systematically absent and redundant data left 3354 unique data in the final data set.

The structure was solved by Patterson methods and refined via standard least-squares and Fourier techniques. In a difference Fourier map calculated following the refinement of all non-hydrogen atoms with anisotropic thermal parameters, peaks were found corresponding to the positions of all of the hydrogen atoms on the cumulene, and most of the hydrogen atoms on the (η^5-C_5Me_5) ligands. Hydrogen atoms were assigned idealized locations and values of B_{iso} approximately 1.15 to 1.3 times the B_{eqv} of the atoms to which they were attached. They were included in structure factor calculations, but not refined.

The residuals for 281 variables refined against the 2561 data for which $F^2 > 3\sigma F^2$ were R = 2.49%, wR = 2.91%, and GOF = 1.713. The R value for all 3354 data was 5.74%. In the final cycles of refinement a secondary extinction parameter[21] was included (maximum correction 8% on F).

The quantity minimized by the least squares was $\sum w(F_o - F_c)^2$, where w is the weight of a given observation. The p-factor, used to reduce the weight of intense reflections, was set to 0.02 in the last cycles of refinement. The analytical forms of the scattering factor tables for the neutral atoms were used and all scattering factors were corrected for both the real and imaginary components of anomalous dispersion.

Inspection of the residuals ordered in ranges of sin (θ)/λ, F_o, and parity and value of the individual indexes showed no unusual features or trends. The largest peak in the final difference Fourier map had an electron density of 2.35 e$^-$/Å^3, and the lowest excursion −1.30 e$^-$/Å^3. All major peaks and valleys were located near the iridium atoms.

The positional parameters of the non-hydrogen atoms are given in Table VI. Other crystallographic data are provided as supplementary information.

Table VI. Positional Parameters for **20** and Their Estimated Standard Deviations

atom	x	y	z	B (Å^2)
Ir1	0.19261 (1)	0.02214 (4)	0.23158 (2)	2.602 (6)
Ir2	0.31567 (1)	0.03325 (4)	0.15124 (2)	2.903 (7)
C1	0.2593 (4)	0.1996 (9)	0.2356 (5)	3.0 (2)
C2	0.2469 (4)	0.353 (1)	0.2091 (6)	4.0 (2)
C3	0.2926 (5)	0.469 (1)	0.2233 (6)	4.8 (2)
C4	0.3572 (5)	0.438 (1)	0.2641 (7)	5.1 (2)
C5	0.3752 (4)	0.293 (1)	0.2863 (6)	4.8 (2)
C6	0.3280 (4)	0.1669 (9)	0.2732 (5)	3.0 (2)
C7	0.3394 (4)	0.0063 (9)	0.2889 (5)	3.3 (2)
C8	0.2800 (4)	−0.080 (1)	0.2733 (5)	3.6 (2)
C9	0.4050 (4)	−0.064 (1)	0.3273 (6)	4.9 (2)
C11	0.1076 (4)	−0.140 (1)	0.2570 (6)	4.0 (2)
C12	0.1034 (4)	−0.0068 (9)	0.3103 (5)	3.2 (2)
C13	0.0908 (4)	0.120 (1)	0.2534 (6)	4.0 (2)
C14	0.0889 (4)	0.070 (1)	0.1666 (6)	5.3 (2)
C15	0.0998 (4)	−0.095 (1)	0.1695 (6)	5.5 (2)
C16	0.1168 (5)	−0.302 (1)	0.2909 (9)	8.2 (4)
C17	0.1039 (6)	−0.003 (2)	0.4088 (7)	7.7 (3)
C18	0.0786 (5)	0.284 (1)	0.284 (1)	8.7 (4)
C19	0.0699 (5)	0.166 (2)	0.0865 (7)	11.3 (4)
C20	0.0955 (5)	−0.207 (2)	0.0930 (8)	12.5 (4)
C21	0.3148 (4)	−0.099 (1)	0.0311 (5)	4.4 (2)
C22	0.2990 (5)	0.052 (1)	0.0093 (5)	4.3 (2)
C23	0.3563 (5)	0.147 (1)	0.0369 (5)	5.1 (2)
C24	0.4091 (4)	0.043 (1)	0.0752 (6)	4.1 (2)
C25	0.3817 (4)	−0.107 (1)	0.0709 (5)	4.4 (2)
C26	0.2721 (6)	−0.241 (1)	0.0072 (7)	7.5 (3)
C27	0.2357 (6)	0.108 (2)	−0.0406 (7)	8.5 (4)
C28	0.3646 (7)	0.316 (1)	0.0258 (8)	9.9 (4)
C29	0.4791 (5)	0.088 (2)	0.1109 (7)	7.0 (3)
C30	0.4198 (5)	−0.252 (1)	0.1008 (7)	6.6 (3)

Synthesis of (η^5-C_5Me_5)Ir(η^3-C_3H_5)R: R = c-C_6H_{11} (21). In the drybox 100 mg (0.248 mmol) of the (π-allyl)iridium chloride **1** was weighed into a 50-mL round-bottomed flask and 20 mL of diethyl ether was added, giving a yellow solution. To this solution was added c-$C_6H_{11}MgCl$ (0.16 mL, 2 M, 0.32 mmol) dropwise via syringe. The reaction mixture was allowed to stir for 24 h during which time the solution turned clear and a white solid formed. The crude reaction mixture was quenched by rapid filtration through a short pad of alumina, packed in a medium pore frit, using ca. 25 mL of diethyl ether. The filtrate was concentrated in vacuo giving a white residue. Crystallization from pentane at −40 °C in the drybox freezer gave 64 mg (0.14 mmol, 57% yield) of analytically pure, clear crystals of **21**: mp 125–126 °C; IR (KBr) 3040 (m), 2971 (s), 2916 (s), 2842 (s), 2822 (m), 1477 (m), 1458 (m), 1442 (m), 1380 (s), 1029 (m), 993 (m), 951 (m), 598 (w); ^1H NMR (C_6D_6) δ 3.23 (m, 1 H), 2.85 (d, J = 6.5 Hz, 2 H), 2.1–1.8, 1.7–1.3 (m, CH_2's of cyclohexyl group), 1.58 (s, 15 H), 1.08 (d, J = 8.8 Hz, 2 H), 0.50 (t, J = 12 Hz), α-H of cyclohexyl ligand, determined by $^1H/^{13}C$ heteronuclear 2-D NMR spectroscopy; ^{13}C NMR (C_6D_6) δ 91.8

(20) For a description of the instrumentation used and a summary of the equations used in data analysis, see: Hersh, W. H.; Hollander, F. J.; Bergman, R. G. *J. Am. Chem. Soc.* **1983**, *105*, 5831.

(21) Zachariesen, W. H. *Acta Crystallogr.* **1963**, *16*, 1139.

(s), 69.4 (d, J = 160.2 Hz), 39.6 (t, J = 123.6 Hz), 37.1 (t, J = 156 Hz), 32.7 (t, J = 122.5 Hz), 28.5 (t, J = 128 Hz), 24.3 (d, J = 130 Hz), 9.05 (q, J = 127.1 Hz); mass spectrum, m/e 452, 367 (M^+, base). Anal. Calcd for $C_{19}H_{31}Ir$: C, 50.55; H, 6.87. Found: C, 50.38; H, 7.00.

R = CH_3 (22). Replacing (cyclohexyl)MgCl with CH_3MgCl in the synthesis of **21** gave the allylmethyliridium complex **22** in 60% yield after crystallization from pentane at −40 °C: mp 86.5–87 °C; ^1H NMR (C_6D_6) δ 3.42 (m, 1 H), 2.86 (d, J = 6.2 Hz, 2 H), 1.58 (s, 15 H), 1.33 (d, J = 8.9 Hz, 2 H), 0.73 (s, 3 H); ^{13}C NMR (C_6D_6) δ 91.17 (s), 69.3 (d, J = 162 Hz), 35.0 (t, J = 159.6 Hz), 8.7 (q, J = 156.8 Hz), −16.0 (q, J = 127 Hz); mass spectrum, m/e 384, 367 (M^+, base). Anal. Calcd for $C_{14}H_{23}Ir$: C, 43.86; H, 6.00. Found: C, 43.72; H, 6.10.

R = $CH_2C_6H_5$ (23). Use of (benzyl)MgCl in place of (cyclohexyl)-MgCl gave **23** in 60.5% yield after crystallization from pentane at −40 °C: ^1H NMR (C_6D_6) δ 7.29 (d, J = 7.2 Hz, 2 H), 7.19 (t, J = 7.4 Hz, 2 H), 7.03 (br t, J = 7.1 Hz, 1 H), 3.36 (m, 1 H), 2.90 (s, 2 H), 2.78 (d, J = 6.3 Hz, 2 H), 1.41 (s, 15 H), 1.40 (obscured, 2 H); ^1H NMR (acetone-d_6) δ 7.0 (m, 4 H), 6.8 (m, 1 H), 3.5 (m, 1 H), 2.68 (d, J = 6.5 Hz, 2 H), 2.56 (s, 2 H), 1.70 (s, 15 H), 0.96 (d, J = 8.9 Hz, 2 H); $^{13}C\{^1H\}$ NMR (acetone-d_6) δ 153.1 (s), 129.5 (s), 127.8 (s), 122.8 (s), 92.4 (s), 71.1 (s), 36.7 (s), 8.7 (s), 5.4 (s); mass spectrum, m/e 460, 367 (M^+, base). Anal. Calcd for $C_{20}H_{27}Ir$: C, 52.29; H, 5.88. Found: C, 51.99; H, 5.90.

R = C_6H_5 (24). Use of PhMgCl in place of (cyclohexyl)MgCl and crystallization at −40 °C from a toluene/hexane mixture gave the phenyl allyl analogue **24** in 86% isolated yield: mp 147.5–148 °C; ^1H NMR (C_6D_6) δ 7.51 (m, 2 H), 7.2–7.0 (m, 3 H), 3.52 (m, 1 H), 2.99 (d, J = 6.3 Hz, 2 H), 1.91 (d, J = 9.2 Hz, 2 H), 1.47 (s, 15 H), ^1H NMR (acetone-d_6) δ 7.22 (br d, J = 6.8 Hz, 2 H), 6.8–6.65 (m, 3 H), 3.69 (m, 1 H), 2.97 (d, J = 6.5 Hz, 2 H), 1.75 (s, 15 H), 1.45 (d, J = 9.2 Hz, 2 H); ^{13}C NMR (acetone-d_6) δ 145.6 (s), 143.8 (s), 127.8 (s), 121.8 (s), 93.3 (s), 73.7 (s), 36.7 (s), 9.1 (s); mass spectrum, m/e 446, 429 (M^+, base). Anal. Calcd for $C_{19}H_{25}Ir$: C, 51.21; H, 5.62. Found: C, 51.40; H, 5.73.

Thermolysis of 21 in C_6H_6. In the drybox 46 mg (0.102 mmol) of **21** and ca. 5 mL of C_6H_6 were added to a glass bomb. The bomb was sealed, removed to the vacuum line, and then degassed. The clear solution was heated to 120 °C in an oil bath for 10 h during which time the solution gradually darkened. The volatile materials were removed in vacuo leaving a dark residue which was dissolved in pentane and then cooled to −40 °C in the drybox freezer giving a white powder. By ^1H NMR analysis the product from this reaction is the phenyl allyl complex **24** (25 mg, 0.056 mmol, 55% yield).

Thermolysis of 21 in C_6D_6. In the drybox ca. 10 mg of the cyclohexyl allyl complex **21** and 0.6 mL of C_6D_6 were added to a NMR tube which was fused to a ground glass joint. The tube was fitted with a Kontes vacuum stopcock, removed to the vacuum line, and the solution was degassed. The NMR tube was flame sealed under vacuum and then the reaction materials were heated to 120 °C for 7.5 h. The reaction was monitored by ^1H NMR spectroscopy and showed the clean formation of **24**-d_6 and free cyclohexane (δ 1.39 ppm). There was no observable formation of **24**-d_5 by ^1H NMR spectroscopy. For **24**-d_6: ^1H NMR (C_6D_6) δ 3.0 (br s, 2 H), 1.92 (br s, 2 H), 1.47 (s, 15 H).

Thermolysis of Methyl Allyl and Benzyl Allyl Complexes 22-23 in C_6D_6. Solutions of **22** and **23** in C_6D_6 were prepared in NMR tubes as described above. Thermolysis of the methyl allyl complex **22** at 175 °C for 4 h gave **24**-d_6 and **24**-d_5 in a 2:1 ratio, determined by comparison of the integrated ratios of proton resonances for the α- and β-allylic positions; CH_4 was also detected (δ 0.147 ppm) by ^1H NMR spectroscopy. Thermolysis of the benzyl allyl complex at 150 °C for 15 h produced **24**-d_6 and **24**-d_5 in a 3.7:1 ratio; determined as above: toluene was also detected (δ 2.90, CH_3).

Synthesis of (η^5-C_5Me_5)Ir(PMe_3)(C_6D_5)(*n*-C_3H_6D) (3-d_6). In the drybox 70 mg (0.190 mmol) of **2** and 2 mL of C_6D_6 were added to a Pyrex bomb. The bomb was then transferred to a vacuum line and the solution degassed. To the solution was added PMe_3 (0.30 mmol) via vacuum transfer. The bomb was wrapped with aluminum foil and then heated to 65 °C for 7 h. The volatile materials were removed in vacuo leaving a white residue which was crystallized from pentane at −40 °C giving 62 mg of **3**-d_6 (0.117 mmol, 62% yield): ^1H NMR (C_6D_6) δ 1.65–1.2 (*n*-propyl group), 1.49 (d, J_{HP} = 1.8 Hz, 15 H), 1.06 (d, J_{HP} = 9.6 Hz); $^{13}C\{^1H\}$ NMR (C_6D_6, see Figure 4 for assignments) δ 139.4 (t, J_{CD} = 23.3 Hz), 136.9 (d, J_{CP} = 12.4 Hz), 126.7 (t, J_{CD} = 23.5 Hz), 120.8 (t, J_{CD} = 23.3 Hz), 93.1 (d, J_{CP} = 3.2 Hz), 30.0 (d, J_{CP} = 5.1 Hz), 29.7 (dt, J_{CP} = 4.8 Hz, J_{CD} = 19 Hz), 21.4 (s), 21.35 (s), 21.15 (t, J_{CD} = 18.9 Hz), 15.34 (d, J_{CP} = 35.6 Hz), 9.2 (s), 5.15 (d, J_{CP} = 9.1 Hz), 5.07 (d, J_{CP} = 8.2 Hz), 4.95 (m); $^2H\{^1H\}$ NMR (C_6H_6) δ 7.4 (br s), 7.2 (br s), 1.55 (br s), 1.46 (br s), 1.38 (br s), 1.24 (br s); $^{31}P\{^1H\}$ NMR (C_6D_6) δ −40.18; mass spectrum, m/e 530, 486, 403 (M^+, $M^+ - C_3H_6D$, base).

(η^5-C_5Me_5)Ir(PPh_3)(C_6D_5)*n*-C_3H_6D (4-d_6). In the drybox 60 mg (0.163 mmol) of **2**, 60 mg (0.23 mmol) of PPh_3, and 1.5 mL of C_6D_6 were added to a Pyrex bomb. The bomb was removed to a vacuum line and the solution was degassed. The reaction mixture was heated to 65 °C for 5.25 h during which time the solution turned a pale yellow. The volatile materials were removed in vacuo leaving a light yellow solid. This residue was crystallized from toluene/hexane (1:1) giving 66 mg (0.092 mmol, 57% yield) of **4**-d_6: ^1H NMR (CD_2Cl_2) δ 7.4–7.2 (br, PPh_3), 1.49 (d, J_{HP} = 1.4 Hz, 15 H), 1.5–1.24, 1.15–1.05, 0.85–0.7, 0.5–0.4 (br m, *n*-propyl); $^2H\{^1H\}$ NMR (CD_2Cl_2) δ 6.74 (br s), 1.38 (br s), 1.08 (br s), 0.73 (br s), 0.47 (br s); $^{13}C\{^1H\}$ NMR (CD_2Cl_2) δ 139.2 (t, J_{CD} = 24.3 Hz), 135–127 (br, PPh_3), 132.5 (d, J_{CP} = 12 Hz), 125.9 (t, J_{CD} = 22.6 Hz), 120.4 (t, J_{CD} = 22.6 Hz), 30.0 (s), 29.7 (t, J_{CD} = 20.0 Hz), 20.6 (s), 20.5 (s), 20.3 (t, J_{CD} = 19.1 Hz), 11.3 (d, J_{CP} = 8.4 Hz), 11.2 (d, J_{CP} = 8.8 Hz), 11.0 (m), 9.2 (s); $^{31}P\{^1H\}$ NMR (CD_2Cl_2) δ 15.21; mass spectrum, m/e 716, 672, 83 (M^+, $M^+ - C_3H_6D$, base).

Rate Dependence on PPh_3 Concentration. In the drybox 8–10 mg of **2**, 3 mg of ferrocene (as an internal standard), and an accurately weighed amount of PPh_3 was added to an NMR tube which was fused to a ground glass joint. To this mixture was added 0.60 mL of C_6D_6 via syringe. The NMR tube as fitted with a Kontes vacuum stopcock and the apparatus was removed to a vacuum line. The solution was degassed and then the tube was flame sealed under vacuum. The NMR tube was heated to 45 °C in a water bath and the rate of disappearance of **2** was monitored by integration of the (η^5-C_5Me_5) ligand in **2** versus ferrocene. This procedure was repeated for a total of five different concentrations of PPh_3. The rate of disappearance of **2** was first order in **2** in all cases (see Table II for data).

Rate Dependence on Concentration of PMe_3. In the drybox 8–10 mg of **2**, 3 mg of ferrocene, and 0.60 mL of C_6D_6 were added to an NMR tube fused to a ground glass joint. The tube was fitted with a Kontes vacuum stopcock and then removed to a vacuum line. The solution was degassed and PMe_3 added by vacuum transfer. The amount of PMe_3 added was established by integration of the PMe_3 resonance versus ferrocene in the ^1H NMR spectrum. The rate of disappearance of **2** was monitored by ^1H NMR spectroscopy through at least 3 half-lives and gave clean first-order decay plots in all cases (see Table II).

Rate Dependence on Concentration of C_6R_6 (R = H and D). In the drybox 8–10 mg of **2**, 20–25 mg of PPh_3, and 3 mg of ferrocene were added to a NMR tube which was fused to a ground glass joint. To this mixture was added various concentrations of C_6R_6 (made by dilution of a stock solution of 4 M C_6R_6 in C_6D_{12} with C_6D_{12}). In all cases the final volume was 0.60 mL. The NMR tube was fitted with a Kontes vacuum stopcock and then removed to a vacuum line. The solution was degassed and the tube was flame sealed under vacuum. Again the reaction was followed by integration of the (η^5-C_5Me_5) ligand versus ferrocene through at least 3 half-lives and in all cases clean first-order decay of **2** was observed (Table III and Figure 3a,b).

Thermolysis of 2 in C_6H_6/C_6D_6 with Added PMe_3. In the drybox 26 mg (0.070 mmol) of **2**, 0.80 mL of C_6H_6, and 0.80 mL of C_6D_6 were added to a Pyrex bomb. The bomb was removed to a vacuum line, and the solution was degassed. Into this solution was vacuum transferred 0.15 mmol of PMe_3. The solution was heated to 45 °C for 14 h followed by the removal of volatile materials. The residue was dissolved in C_6D_6 and by integration of the trimethylphosphine resonance versus the ortho-aromatic resonances in the ^1H NMR spectrum a ratio of 1.18 ± 0.1 (normalized per hydrogen) was obtained. The reaction was repeated two more times giving a ratio of C–H versus C–D insertion of 1.2 ± 0.02.

Thermolysis of 2 in 1,3,5-$C_6D_3H_3$ with Added PMe_3. In the drybox 14 mg (0.038 mmol) of **2** and 1.0 mL of 1,3,5-$C_6D_3H_3$ were added to a Pyrex bomb. The bomb was removed to a vacuum line and the solution was degassed. Into the solution was vacuum transferred 0.075 mmol of PMe_3. The reaction mixture was heated to 45 °C for 14 h followed by the removal of the volatile materials. The residue was dissolved in THF-d_8 and a ^1H NMR spectrum was taken. Integration of the meta-aromatic resonance versus the ortho-aromatic resonance gave a ratio of 1.30:1. This reaction was repeated two more times giving a ratio of C–H versus C–D insertion of 1.28 ± 0.04. ^1H NMR (THF-d_8) δ 7.15 (s, 1 H), 6.73 (s, 1 H), 6.67 (s, 1 H), 1.60 (d, J_{HP} = 1.6 Hz, 15 H), 1.36 (d, J_{HP} = 9.6 Hz, 9 H), 1.6–1.25 (m, CH_2's of *n*-propyl), 0.99 (CH_3); mass spectrum, m/e 527, 403 (M^+, base).

Thermolysis of 2 in C_6D_6. In the drybox 28 mg (0.076 mmol) of **2** and 2 mL of C_6D_6 were added to a Pyrex bomb. The bomb was removed to a vacuum line and the solution was degassed. The bomb was wrapped in aluminum foil and then heated to 45 °C for 24 h during which time the solution turned dark brown. The volatile materials were removed in vacuo leaving a dark oily residue which was extracted into pentane in the drybox. The pentane solution was filtered into a sublimation apparatus and then concentrated. The product was sublimed at ca. 40 °C and 10^{-4} Torr giving a white solid in 60% yield (17 mg, 0.045 mmol) that was

identified as **2**-d_6: IR (KBr) 2978 (s), 2956 (s), 2904 (s), 2299 (m), 2178 (m), 2099 (w), 1513 (s, Ir–D), 1475 (s), 1454 (s), 1425 (m), 1383 (s), 1355 (s), 1205 (m), 1040 (m), 840 (m), 584 (s), 464 (s); ^{1}H NMR (C_6D_6) δ 1.86 (s); ^{2}H NMR (C_6H_6) δ 2.94 (s, 1 D), 2.53 (s, 2 D), 2.24 (s, 2 D), −16.7 (s, 1 D); ^{13}C{^{1}H} NMR (C_6D_6) δ 91.4 (s), 10.57 (s); mass spectrum, m/e 376 (M^+ and base).

Kinetics of Reaction between 2-d_6, C_6D_6, and PPh_3. In the drybox 6–8 mg of **2**-d_6, 20–25 mg of PPh_3, 3 mg of ferrocene, and various concentrations of C_6D_6 (made by dilution of a 4 M solution of C_6D_6 in C_6D_{12} with C_6D_{12}) were added to a NMR tube fused to a glass joint. In all cases the total volume was 0.60 mL. The tube was fitted with a Kontes vacuum stopcock and then removed to a vacuum line. The solution was degassed and the tube was flame sealed under vacuum. The rate of disappearance of **2**-d_6 was monitored by ^{1}H NMR spectroscopy and gave clean first-order decay plots in all cases (see Table IV and Figure 3a,b). The product of the reaction between **2**-d_6, PPh_3, and C_6D_6 was isolated and identified as **4**-d_{12}: ^{1}H NMR (C_6D_6) δ 7.6–7.3 (br, PPh_3), 7.1–6.9 (br, PPh_3), 1.46 (d, J_{HP} = 1.6 Hz); ^{31}P{^{1}H} NMR (C_6D_6) δ 15.49; mass spectrum, m/e 722, 672, 262 (M^+, $M^+ - C_3D_7$, base).

Synthesis of (η^5-C_5Me_5)Ir(η^3-C_3H_5)$^-$Li$^+$ (25). In the drybox 82 mg (0.222 mmol) of the (π-allyl)iridium hydride **2** was weighed into a 50-mL round-bottomed flask. To this was added 20 mL of pentane followed by the dropwise addition of 160 μL (1.7 M) of t-BuLi via syringe. The reaction was allowed to stir for 24 h during which time the solution first turned yellow followed by the deposition of a green solid. The crude reaction was cooled in the drybox freezer (ca. −40 °C). The green solid was collected by filtration and then washed with pentane giving 62 mg (0.165 mmol, 74% yield) of analytically pure **25**: ^{1}H NMR (THF-d_8) δ 2.41 (m), 1.99 (s), 1.50 (d, J = 3.5 Hz), −1.38 (br s); ^{13}C{^{1}H} NMR (THF-d_8) δ 84.46 (s), 40.61 (s), 12.13 (s), 5.88 (s). Anal. Calcd for $C_{13}H_{20}IrLi$: C, 41.58; H, 5.33; Li, 1.85. Found: C, 41.73; H, 5.44; Li, 1.78.

Synthesis of (η^5-C_5Me_5)Ir(η^3-C_3H_5)D (2-d_1). In the drybox 58 mg (0.157 mmol) of **2** was weighed into a 50-mL round-bottomed flask. To this was added 10 mL of pentane followed by the dropwise addition of 140 μL (1.7 M) of t-BuLi. The reaction mixture was allowed to stir for 28 h during which time the solution first turned yellow and then a green solid deposited. To this green slurry was added an excess of MeOD, upon which the solution cleared. The reaction mixture was allowed to stir for 15 min followed by removal of the volatile materials in vacuo. The residue was extracted into pentane, filtered, and concentrated giving a white solid which was pure by ^{1}H NMR (47 mg, 0.127 mmol, 81% yield). IR (KBr) 3047 (m), 2982 (s), 2909 (s), 1514 (s, Ir–D), 1475 (s), 1383 (s), 1201 (w), 1073 (w), 1039 (m), 806 (m), 639 (m), 584 (m), 470 (m); ^{1}H NMR (C_6D_6) δ 2.95 (m, 1 H), 2.54 (d, J = 5.6 Hz, 2 H), 2.23 (d, J = 8.9 Hz, 2 H), 1.85 (s, 15 H); ^{1}H NMR (C_6D_{12}) δ 2.79 (m, 1 H), 2.24 (d, J = 5.7 Hz, 2 H), 2.02 (s, 15 H), 1.74 (d, J = 8.8 Hz); ^{2}H NMR (C_6H_6) δ −16.6 (s); mass spectrum (10 eV), m/e 371, 369 (M^+, $M^+ - H_2$ and base).

Thermolysis of 2-d_1. In the drybox 61 mg (0.165 mmol) of **2**-d_1 and 3 mL of C_6D_{12} were added to a glass bomb. The bomb was sealed with a Kontes vacuum stopcock and removed to a vacuum line. The solution was degassed and was heated to 45 °C for 17.5 h. The volatile materials were removed in vacuo, the residue was taken up in C_6H_6, and the following ^{2}H NMR spectrum was recorded: ^{2}H NMR (C_6H_6) δ 2.51 (s), 2.21 (s), −16.6 (s). Integration of the α-allylic deuterium resonances versus the Ir–D resonance gave (after correction for the 4:1 statistical preference for the terminal allylic positions) a K_{eq} value of 2.2 ± 0.14. Further heating in C_6D_{12} caused no further change in K_{eq}.

Acknowledgment. This work was supported by the Director, Office of Basic Energy Research, Office of Basic Energy Sciences, Chemical Sciences Division of the U.S. Department of Energy under Contract DE-AC03-76SF00098. W.D.M. thanks the Organic Division of the American Chemical Society for a graduate fellowship. The crystal structure analysis was performed by Dr. F. J. Hollander, staff crystallographer at the UC Berkeley X-ray crystallographic facility (CHEXRAY). We are grateful to the Johnson-Matthey Corp. for a generous loan of iridium chloride. Partial funding for the equipment in the Berkeley NMR facility was provided by the National Science Foundation through Grant No. CHE79-07027. The Bruker AM-500 NMR spectrometer was purchased with funds from NSF (No. CHE-8208994) and NIH (No. RR-02428) equipment grants.

Registry No. 1, 96427-39-3; **2**, 96427-40-6; **2**-d_1, 114378-66-4; **2**-d_6, 114378-62-0; **3**, 96427-48-4; **3**-Ph-d_3, 114378-64-2; **3**-Ph-d_2-Pr-d_1, 114378-69-7; **3**-d_6, 114378-67-5; **4**, 114378-40-4; **4**-d_6, 114378-68-6; **4**-d_{12}, 114378-63-1; **5**, 114378-41-5; **6**, 96427-47-3; **7**, 114378-42-6; **8a**, 114378-43-7; **8b**, 114421-14-6; **9**, 114378-44-8; **10**, 114378-45-9; **11**, 114378-46-0; **12**, 114378-47-1; **13**, 114378-48-2; **14**, 114378-49-3; **15** isomer 1, 114378-50-6; **15** isomer 2, 114421-15-7; **16** isomer 1, 114378-51-7; **16** isomer 2, 114421-16-8; **17** isomer 1, 114378-52-8; **17** isomer 2, 114421-17-9; **18**, 114378-53-9; **19**, 114378-54-0; **20**, 114378-55-1; **21**, 114378-56-2; **22**, 114378-57-3; **23**, 114378-58-4; **24**, 114378-59-5; **24**-d_5, 114378-61-9; **24**-d_6, 114378-60-8; **25**, 114378-65-3; (η^5-C_5Me_5)Ir(PMe$_3$)Br$_2$, 85453-01-6; (η^5-C_5Me_5)Ir(η^3-1-MeC_3H_4)Cl, 32660-86-9; (η^5-C_5Me_5)Ir(PMe$_3$)$_2$H$^+$BF$_4^-$, 96096-85-4; [(η^5-C_5Me_5)IrCl$_2$]$_2$, 12354-84-6; 1,3,5-$C_6D_3H_3$, 1684-47-5; C_6H_6, 71-43-2; *n*-butane, 106-97-8; cyclopropane, 75-19-4; *trans*-2-butene, 624-64-6; *cis*-2-butene, 590-18-1; *n*-propylbenzene, 103-65-1; cumene, 98-82-8.

Supplementary Material Available: Further details of the structure determination of complex **20** including tables of general temperature factor expressions and least-squares planes (10 pages); tables of calculated and observed structure factors (20 pages). Ordering information is given on any current masthead page.